Delay characterization of multi-hop transmission in a Poisson field of interference

Kostas Stamatiou and Martin Haenggi, *Senior Member, IEEE*

***Abstract*—We evaluate the end-to-end delay of a multi-hop transmission scheme that includes a source, a number of relays and a destination, in the presence of interferers located according to a Poisson point process. The medium-access control (MAC) protocol considered is a combination of TDMA and ALOHA, according to which nodes located a certain number of hops apart are allowed to transmit with a certain probability. Based on an independent transmissions assumption, which decouples the queue evolutions, our analysis provides explicit expressions for the mean end-to-end delay and throughput, as well as scaling laws when the interferer density grows to infinity. If the source always has packets to transmit, we find that full spatial reuse, i.e., ALOHA, is asymptotically delay-optimal, but requires more hops than a TDMA-ALOHA protocol.**

The results of our analysis have applications in delay-minimizing joint MAC/routing algorithms for networks with randomly located nodes. We simulate a network where sources and relays form a Poisson point process, and each source assembles a route to its destination by selecting the relays closest to the optimal locations. We assess both theoretically and via simulation the sensitivity of the end-to-end delay with respect to imperfect relay placements and route crossings.

***Index Terms*—Multi-hop, end-to-end delay, throughput, Poisson point process, queueing.**

I. Introduction

The main question pertinent to wireless multi-hop networks is determining the delay at which a certain throughput can be achieved, at the end-to-end level. The question is related to the following fundamental tradeoff: On the one hand, a smaller hopping distance provides more robustness to interference and noise, resulting in better link reliability; on the other hand, each node that is added between the source of packets and their final destination also incurs additional delay, as a packet typically has to wait in line before it is transmitted to the next node [1]. The treatment of the problem depends on a number of diverse factors, among which are the employed routing and medium-access (MA) control (MAC) protocols, the channel model and, quite importantly, the topology of the network.

This paper obtains concrete end-to-end delay and throughput results for multi-hop networks with randomly placed nodes, taking into full account the effects of fading, interference and queueing delays due to packet buffering. We optimize the delay over the number of hops between the source of packets and their destination, and other network parameters; obtain asymptotic delay-throughput tradeoffs as the density of nodes goes to infinity; and propose a delay-optimal routing algorithm for networks with randomly placed nodes.

A. Related work and motivation

The delay and throughput of multi-hop networks has been a topic of intense investigation, in particular in the last decade [1]–[4]. An important line of work, spurred by [5], considers the network as a collection of m nodes randomly distributed in a unit-area disk, where source-destination pairs are randomly formed, and focuses on obtaining asymptotic results as m grows large. Following [5] and a number of other papers that dealt exclusively with the issue of achievable throughput (see [2] for an overview), [3] raised the question of delay-constrained throughput. In particular, under an ideal scheme that can schedule transmissions throughout the network, they showed that, for almost all network realizations, the optimal delay-throughput tradeoff is given by $D(m) = \Theta(mT(m))$, where $D(m)$ and $T(m)$ are the delay and throughput scaling, respectively. A similar result was derived in [6], albeit within a different framework where nodes were allowed to move throughout the network in an independent and identically distributed (iid) fashion.

Although useful in shedding light on fundamental performance trends, the previous approach falls short in providing concrete results for given design choices, which are based on realistic routing and MAC protocols. In [7], it was argued that a functional network capacity theory should take into account issues of delay and overhead, since these dramatically affect the performance of practical networks. An approach pioneered in [8] was to consider the network as a collection of transmitters, each with a distinct receiver, which are distributed on the plane as a Poisson point process (PPP). The PPP framework is well suited for networks with no particular structure and uncoordinated transmissions, i.e., a random access MAC (ALOHA). A significant amount of work has been devoted to the study of single-hop PPP networks (see [9] for a comprehensive overview) and the evaluation of metrics such as the expected packet progress [8], the transmission capacity [10] and the spatial density of progress [11].

Given the tractability of the PPP framework, some extensions have been proposed to accommodate multi-hop transmission. In [12], an opportunistic routing strategy was advocated where the relay with the most favorable channel is selected in each hop, and the end-to-end delay was evaluated via simulation. In [4], the end-to-end throughput was derived and optimized over the number of hops, assuming that in each hop the interferer locations are drawn independently according to a PPP. The authors coined the term random-access transport capacity for the optimized throughput, to emphasize that, as in [5], the metric reflects the rate at which

packets are transported from the source to the destination, but in the specific setting where interferer locations and their transmissions are random. In [13], the multi-hop problem was studied from an end-to-end connectivity perspective and bounds were determined on the time required for a path to form between the source and the destination. The common trait of these papers is their "throughput-centric" approach; it is assumed that nodes always have packets to transmit and queueing delays resulting from packet buffering are ignored.

Other related work includes [14]–[19], which have studied the "line network" consisting of a source, a number of relays and a destination. The common assumption here is that the line network operates in a stand-alone fashion, i.e., interference from other such "lines", which are expected to be present in a network environment, is not considered. Assuming a channel model with path-loss, fading and noise, and no delay constraints, [15], [16] determined the end-to-end rate, i.e., the minimum achievable rate over all hops, when a TDMA-access protocol is employed. Alternatively, under a given delay constraint, [17] specified the number of hops and the rate allocation among them, such that the total power consumption is minimized. A similar problem was studied in [14], under an end-to-end success probability requirement. In [19], a decomposition approach was employed to decouple the line network into isolated queues and the end-to-end delay of time-division multiple access (TDMA) and ALOHA protocols was evaluated.

B. Contributions

In this paper, we study the end-to-end delay performance of a multi-hop transmission system (or route, in routing terminology) consisting of a source, a number of relays and a destination, in a network where interferers are located according to a PPP. In this manner, we bridge the gap between existing end-to-end delay results for line networks that do not account for interference [19], and existing end-to-end throughput results for PPP multi-hop networks that do not account for queueing delays [4]. Our main departure point from previous work is the introduction of buffers at the nodes, which leads to the explicit evaluation of the associated packet service and waiting times. The coupling of the queue evolutions renders the evaluation of the end-to-end delay a very challenging problem; consequently, we assume that transmissions across nodes are independent, which allows the use of the framework developed in [20], in order to evaluate the steady-state distribution of the size of each node queue. Section VI-D is devoted to verifying the validity of our approach through simulations.

The MAC protocol considered is a combination of TDMA and ALOHA. In each slot, the protocol schedules nodes which are separated by a given number of hops, and the scheduled nodes are allowed to transmit with a certain probability. It is selected in light of the fact that, in practice, while intra-route coordination is fairly easy, inter-route coordination is hard, hence a random-access policy for scheduled nodes is easily implementable. Moreover, slotted ALOHA arises as a special case, when all nodes in the route are simultaneously scheduled. In this manner, we model and analyze in a "mean sense" a network consisting of an infinite number of mutually interfering routes, which employ the TDMA-ALOHA MAC protocol. We study in detail a scenario where the source always has packets to transmit ("backlogged" source) and show how the analysis can also be adapted for the case of sources with geometric arrivals. In summary, our main contributions consist of:

- Obtaining analytical expressions for the hop success probability and the end-to-end delay as functions of the number of hops, the source MA probability and the intra-route spatial reuse factor.
- Deriving the delay-optimal values of these parameters, and delay-throughput scaling laws when the density of interferers grows to infinity. In particular, it is shown that, in the limit of a large interferer density, maximum intra-route reuse, i.e., slotted ALOHA, minimizes the end-to-end delay.
- Using the theoretically obtained delay-optimal number of hops in order to perform routing in a network where both sources and relays form a PPP. The routing algorithm consists of each source selecting the relays closest to the optimal locations on the source-destination line. We assess theoretically and via simulation the sensitivity of the end-to-end delay with respect to imperfect relay placements and the utilization of given relays by more than one source-destination pairs. Moreover, we verify via a number of experiments the validity of the assumptions that form the backbone of our analysis, in the "small" MA probability regime.

C. Paper outline and notation

In Section II, the system model is described in detail. Section III is devoted to the evaluation of the hop success probability. In Sections IV and V, the mean end-to-end delay is derived and optimized over the relevant network parameters for the cases of backlogged sources and geometric arrivals, respectively. In Section VI, we present our simulation results and in Section VII we summarize our conclusions. Table I includes a list of the main symbols employed throughout the paper. Note that the following conventions are employed for $x \to x_o$: If $\lim_{x\to x_o} f(x) = \lim_{x\to x_o} g(x)$, then $f(x) \approx g(x)$; if $\lim_{x\to x_o} f(x)/g(x) = 1$, then $f(x) \sim g(x)$.

II. System model

A. Topology, source traffic and MAC protocol

A source node employs $N-1$ relays, $N \in \mathbb{N}$, to communicate with a destination at distance R. The relays are placed equidistantly on the source-destination line so that the hopping distance is R/N (if $N = 1$ we have single-hop transmission). A node in the source-destination path is specified by the index $n = 0, \ldots, N$, where $n = 0$ corresponds to the source, $n = 1$ to the first relay and so on.

As in [4], [11], we assume that time is slotted and nodes are synchronized to a common clock. We define the intra-route spatial reuse factor $d = 1, \ldots, N$, which determines the pairwise distance (in hops) between nodes in the route

TABLE I
COMMONLY USED SYMBOLS

Symbol	Meaning
$\Phi(t)$	interferer PPP at time t
$\lambda_{\rm ex}$	interferer density (extrinsic interference)
λ	source density (intrinsic interference)
p_o	source MA probability
p	relay MA probability
ρ	node transmission probability
a	source packet arrival probability (geometric arrivals)
p_s	hop success probability
R	source-destination distance
N	number of hops
$d = 1, \ldots, N$	intra-route spatial reuse factor
γ	spatial contention
$\delta(d)$	intra-route spatial contention
b	propagation exponent
θ	SINR threshold for successful reception

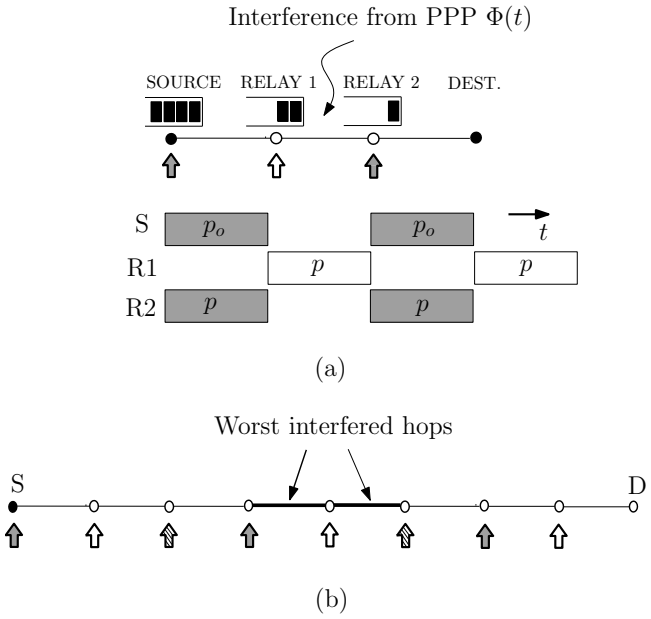

Fig. 1. (a) TDMA-ALOHA MAC protocol with $N = 3$, $d = 2$. In the first slot , the source and the second relay are scheduled ($\mathcal{P}_0 = \{0, 2\}$); in the second slot, the first relay is scheduled ($\mathcal{P}_1 = \{1\}$), and so on. When the source (relay) is scheduled, it accesses the medium with probability p_o (p). If the source is backlogged it always has packets to transmit; if arrivals are geometric, a new packet arrives at the end of its queue every time it is scheduled, with probability a. (b) An example for $N = 8$ and $d = 3$. The worst-interfered hops are 4 and 5, thus $\mathcal{I} = \{-1, 1\}$ and the respective distances are $d + 1 = 4$, $d - 1 = 2$.

that may simultaneously transmit in a slot. By definition, there are d such groups of nodes: $\mathcal{P}_0 = \{0, d, 2d, \ldots\}$, $\mathcal{P}_1 = \{1, d+1, 2d+1, \ldots\}$, $\ldots$, $\mathcal{P}_{d-1} = \{d-1, 2d-1, \ldots\}$. The value $d = 1$ corresponds to maximum intra-route reuse, i.e., a slotted ALOHA protocol, while $d = N$ corresponds to no intra-route reuse, i.e., the case where only one node may transmit at any given time, respectively. When $d < N$, simultaneous transmissions create *intra-route* interference, which, on the average (due to the presence of fading), is larger for smaller values of d.

Each node is equipped with an infinite-capacity buffer[1], where received packets are stored in a first-in first-out fashion. We consider two different cases regarding packet traffic at the source: backlogged, where the source always has packets to transmit, and geometric arrivals, where a new packet arrives at the source buffer with probability a every d slots, i.e., traffic intensity a/d. The first case models a scenario where a large amount of information rests at the source, e.g., a large file in an FTP-type application. The second one models in a simple manner the bursty nature of packet traffic in other types of applications.

The MAC protocol is a combination of TDMA and ALOHA and is described below[2].

1. Set $t = 0$ and randomly select $k \in \{0, \ldots, d-1\}$.
2. Set $\mathcal{P}(t) = \mathcal{P}_k$. If the source is in $\mathcal{P}(t)$, it is *allowed* to transmit with probability p_o. If a relay is in $\mathcal{P}(t)$, it is *allowed* to transmit with probability p.
3. A packet is successfully sent over a hop if the receiver SINR is larger than a threshold θ. If it is not, the transmitting node is informed via an ideal feedback channel and the packet remains at the head of its queue.
4. For geometric arrivals only: If the source is in $\mathcal{P}(t)$, a new packet arrives at the end of its queue with probability a at $t + 1 - \epsilon$, where $1 \gg \epsilon > 0$.
5. Set $t \to t + 1$ and $k \to \mathrm{mod}(k + 1, d)$. Repeat 2-5.

[1]At "low-traffic", the assumption of infinite buffer capacity has negligible impact on the derived results.

[2]The proposed protocol can be implemented in a distributed fashion as follows. Once the route is established, send a test packet to the destination that includes a hop counter. Each relay increases the hop counter by one, thus learning its position and corresponding time slot in the route.

The protocol for both traffic scenarios is depicted in Fig. 1(a), when $N = 3, d = 2$. It is emphasized that a node in $\mathcal{P}(t)$ transmits only when it is allowed to (by the ALOHA part of the MAC) *and* there is at least one packet in its queue. (The two events are equivalent only for the backlogged source.) We denote by ρ_n, $n = 0, \ldots, N-1$, the probability that node n transmits, given that it is scheduled by the TDMA part of the MAC. By definition, $\rho_0 \le p_o$ and $\rho_n \le p,\ n = 1, \ldots, N-1$.

We model network or *inter-route* interference by assuming that, in slot t, the locations of inter-route interferers are drawn from a PPP $\Phi(t)$ of density $\lambda_{\rm PPP}$, where $\{\Phi(t)\}$ are iid across t. We consider two cases, one of *extrinsic* and one of *intrinsic* interference, which are defined below:

Extrinsic interference: $\lambda_{\rm PPP} = \lambda_{\rm ex}$. Inter-route interferers are randomly located on the plane with arbitrary density $\lambda_{\rm ex}$.

Intrinsic interference: $\lambda_{\rm PPP} = \lambda N \bar{\rho}/d$. The network consists of an infinite number of randomly located and mutually interfering routes, whose nodes observe the MAC protocol described above in a slot-synchronous manner. In particular, λ is the density of sources (or routes) in the network, and $N\bar{\rho}/d$ reflects the fact that, with intra-route reuse d, there are on average $N\bar{\rho}/d$ interferers per route, where $\bar{\rho} = N^{-1} \sum_{n=0}^{N-1} \rho_n$. If $d = N$, only one node per route is scheduled at any given slot, so $\lambda_{\rm PPP} = \lambda\bar{\rho}/N$; if $d = 1$, all nodes per route are simultaneously scheduled and $\lambda_{\rm PPP} = \lambda\bar{\rho}$. Since $\lambda_{\rm PPP}$ is proportional to $\bar{\rho}$, we explicitly take into account that an inter-route node is an interferer only when it is allowed to transmit *and* it has at least one packet in its queue.

B. SINR-based packet successes

The channel between two nodes at distance r includes Rayleigh fading and path-loss according to the law r^{-b}, where $b > 2$ is the path-loss exponent. The fading coefficients are spatially iid, with a coherence time that takes values in $[1, d]$ (i.e., the fading is assumed to change at least as frequently as a node is allowed to transmit). All the nodes have the same transmit power and the transmit signal-to-noise-ratio is β.

Suppose that node $n-1$ is scheduled at time t, i.e., $n-1 \in \mathcal{P}(t)$ and its queue is not empty. Without loss of generality, assume that node n is located at the origin. A packet is successfully received by n if

$$\mathrm{SINR}_n(t) \triangleq \frac{A(t)(R/N)^{-b}}{I_{n,\mathrm{o}}(t) + I_{n,\mathrm{i}}(t) + \beta^{-1}} > \theta \tag{1}$$

where

- $A(t)$ is the fading coefficient between $n-1$ and n, exponentially distributed with unit mean.
- $I_{n,\mathrm{o}}(t)$ is the total inter-route interference power

$$I_{n,\mathrm{o}}(t) = \sum_{x \in \Phi(t)} A_x(t)|x|^{-b}, \tag{2}$$

  where $A_x(t)$, exponentially distributed with unit mean, is the fading coefficient between the interferer at location $x \in \Phi(t)$ and n.
- $I_{n,\mathrm{i}}(t)$ is the total intra-route interference power

$$I_{n,\mathrm{i}}(t) = \sum_{m \in \mathcal{P}(t) \setminus \{n-1\}} e_m(t) A_m(t)|x_m|^{-b}, \tag{3}$$

  where $e_m(t) = 1$ if m is a transmitter (and zero otherwise), $A_m(t)$ is the fading coefficient between m and n, and x_m is the location of m.

Note that the reception model based on (1) has an embedded half-duplex constraint. If $d = 1$, $n \in \mathcal{P}(t)$, thus, if $e_n(t) = 1$, $\mathrm{SINR}_n(t) = 0$.

III. A General Expression for the Hop Success Probability

In order to simplify the analysis, we ignore the favorable fact that nodes at the edge of the route are subject to less intra-route interference and assume that the success probabilities are equal to the one of the worst-interfered hop, which we denote by p_s. Due to symmetry, the probabilities of transmission are equal, i.e., $\rho_1 = \cdots = \rho_{N-1} \triangleq \rho$ and $\bar{\rho} = \rho$. In the following proposition, we derive an expression for p_s, under the assumption that transmissions occur *independently* with probability ρ.

Proposition 1 *If nodes scheduled by the TDMA part of the MAC transmit independently with probability ρ, then*

$$p_s = p_{s,\mathrm{o}} \cdot p_{s,\mathrm{i}} \cdot p_{s,\mathrm{n}} \tag{4}$$

where

$$p_{s,\mathrm{o}} = \mathrm{e}^{-\lambda_{\mathrm{PPP}} c \left(\frac{R}{N}\right)^2}, \tag{5}$$

with $c = \Gamma(1+2/b)\Gamma(1-2/b)\pi\theta^{2/b}$,

$$p_{s,\mathrm{i}} = \prod_{i \in \mathcal{I}} \left(1 - \rho + \frac{\rho}{1 + |di-1|^{-b}\theta}\right), \tag{6}$$

with

$$\mathcal{I} = \left\{ -\left\lfloor \frac{1}{2}\left\lceil \frac{N}{d} \right\rceil \right\rfloor, -1, 1, \ldots, \left\lceil \frac{N}{d} \right\rceil - \left\lfloor \frac{1}{2}\left\lceil \frac{N}{d} \right\rceil \right\rfloor - 1 \right\}, \tag{7}$$

and

$$p_{s,\mathrm{n}} = \mathrm{e}^{-\left(\frac{R}{N}\right)^b \theta \beta^{-1}}. \tag{8}$$

Proof: For the proof, we employ the approach in Section III.B of [9]. From (1), the success probability can be written as

$$p_s = \mathbb{P}\left(A(t) \geq \theta (R/N)^b \left(I_{n,\mathrm{o}}(t) + I_{n,\mathrm{i}}(t) + \beta^{-1}\right)\right).$$

Due to the independence of $A(t), I_{n,\mathrm{o}}(t), I_{n,\mathrm{i}}(t)$, and the exponential distribution of $A(t)$, we have that

$$p_s = \mathbb{E}\left[\mathrm{e}^{-\left(\frac{R}{N}\right)^b \theta I_{n,\mathrm{o}}(t)}\right] \mathbb{E}\left[\mathrm{e}^{-\left(\frac{R}{N}\right)^b \theta I_{n,\mathrm{i}}(t)}\right] \mathrm{e}^{-\left(\frac{R}{N}\right)^b \theta \beta^{-1}}. \tag{9}$$

Each term in this product corresponds to the success probability taking into account only inter-route interference ($p_{s,\mathrm{o}}$), intra-route interference ($p_{s,\mathrm{i}}$), and noise ($p_{s,\mathrm{n}}$). Since $\Phi(t)$ is a PPP with density λ_{PPP}, $p_{s,\mathrm{o}}$ is given by (5) (see [9, Eq. (9)]). Moreover, the index of the transmitter with the worst-interfered receiver is $n = \lfloor \frac{1}{2}\lceil \frac{N}{d} \rceil \rfloor$, where $\lceil \frac{N}{d} \rceil$ is the maximum number of concurrently scheduled nodes given N and d. The potential intra-route interferers are thus located at distances $(R/N)|id-1|$, where $i \in \mathcal{I}$ and $\mathcal{I}$ is the set defined in (7). Due to the independence of transmission events, from [21, Eq. (19)], we obtain (6). This concludes the proof. ■

Remarks on Proposition 1:

1. The set $\mathcal{I}$ defined in (7) determines the distances of the intra-route interferers for the worst-interfered hop. In Fig. 1(b), an example is shown for $N = 8,\ d = 3$. When $d = N$, $\mathcal{I} = \emptyset$, and $p_{s,\mathrm{i}} = 1$.
2. The assumption of independent transmission events is made for the sake of analytical tractability as the exact tandem queueing system is a very involved problem [19], [22]. When $d < N$, the queue states are correlated due to (a) intra-route interference, and (b) the common to all scheduled hops interference process $\Phi(t)$. Regarding (a), we maintain that the assumption is reasonable when the nodes are not allowed to transmit often, and this is the regime considered in the rest of the paper; indicatively, $\max\{p_o, p\} \lessapprox 0.1$. Regarding (b), as shown in [23], the spatial correlation coefficient of the interference power resulting from a PPP is zero (under the path-loss and fading model of this paper). This indicates that the dependence between packet successes at a given time slot due to $\Phi(t)$ is very weak. On the grounds of these observations, packet successes, determined by the SINR criterion in (1), are considered independent across n and t. Note that when $d = N$, the independence of packet successes (hence transmission events) is exact, since only one node is scheduled at a time, $\{\Phi(t)\}$ are independent across t and the coherence time of the fading is at most N slots.

Based on (6), we now derive a lower bound to $p_{s,\mathrm{i}}$.

Proposition 2 *If $d < N$, then $p_{s,\mathrm{i}}$ can be lower-bounded as*

$$p_{s,\mathrm{i}} \gtrapprox \mathrm{e}^{-\delta\rho}, \tag{10}$$

where

$$\delta = \sum_{i\in\mathbb{Z}\setminus\{0\}} \left(1 - p + \frac{|di-1|^b}{\theta}\right)^{-1}. \tag{11}$$

The bound is tight for $\rho \to 0$.

Proof: Taking the inverse of (6)

$$p_{s,\mathrm{i}}^{-1} = \prod_{i\in\mathcal{I}} \left(1 + \frac{\rho}{1-\rho+|di-1|^b/\theta}\right).$$

Applying the logarithm to both sides and using the inequality $\log(1+x) < x$, $x > 0$, we obtain that

$$p_{s,\mathrm{i}} > \exp\left(-\rho \sum_{i\in\mathcal{I}} \frac{1}{1-\rho+|di-1|^b/\theta}\right).$$

Since $\rho < p$ and $\mathcal{I} \subset \mathbb{Z}\setminus\{0\}$, (10) follows. When $\rho \to 0$, $p_{s,\mathrm{i}} \to 1$ and $\mathrm{e}^{-\delta\rho} \to 1$, which proves the tightness of the bound. ∎

As shown in Fig. 2, $\mathrm{e}^{-\delta\rho}$ provides a good approximation to $p_{s,\mathrm{i}}$ for sufficiently small values of ρ. For analytical convenience, we (conservatively) set $p_{s,\mathrm{i}} = \mathrm{e}^{-\delta\rho}$ when $d < N$. Since $p_{s,\mathrm{i}} = 1$ for $d = N$, from (4), we have the following general expression for p_s, which is employed throughout the rest of the paper,

$$p_s = \exp\left(-\lambda_{\mathrm{PPP}} c \left(\frac{R}{N}\right)^2 - \delta'\rho - \left(\frac{R}{N}\right)^b \theta\beta^{-1}\right), \tag{12}$$

where $\delta' = \delta$ for $d < N$ and $\delta' = 0$ for $d = N$. Based on (12), we define the parameter $\gamma \triangleq \partial p_s/\partial\rho|_{\rho=0}$ as the *spatial contention* [24]. It measures how steeply the success probability decreases with the transmission probability ρ. If $d < N$, $\gamma = \delta$ for $\lambda_{\mathrm{PPP}} = \lambda_{\mathrm{ex}}$, and $\gamma = \lambda c R^2/(Nd) + \delta$ for $\lambda_{\mathrm{PPP}} = \lambda N\rho/d$. In the latter case, i.e., intrinsic interference, γ consists of both an inter- and an intra- route component. Hence, δ is termed the *intra-route spatial contention*, which, as seen from (11), is a decreasing function of d. In order to emphasize the dependence of δ on d, we also employ the notation $\delta(d)$. Note that, if $d = N$, $\gamma = \lambda c R^2/N^2$ for intrinsic interference.

Armed with (12), in the next two sections we examine separately the cases of a backlogged source and geometric arrivals. In each case, we evaluate ρ, derive expressions for the mean end-to-end delay and throughput, and minimize the delay over the relevant network parameters. Since the noise-dependent term in (12) does not depend on ρ, in the remainder of the paper, we focus on the interference-limited regime, i.e., we let $\beta \to \infty$ ($p_{s,\mathrm{n}} = 1$). Closing, in Table II, we have listed and commented on the main assumptions made in this section, which provide the backbone for (12) and the analysis of the following sections. The validity of each assumption is checked via simulation in Section VI-D; Table II also lists the figures where the respective results can be found.

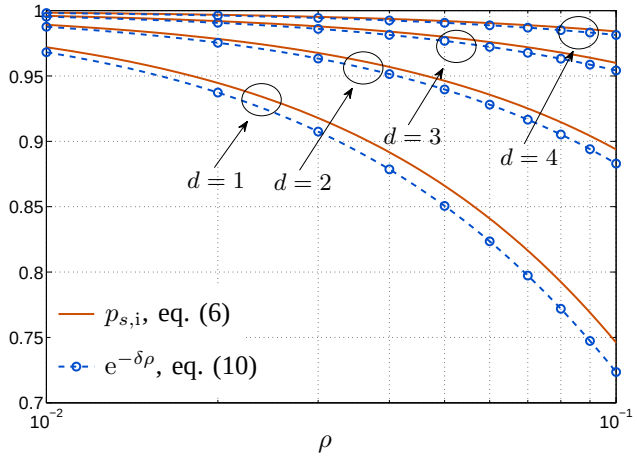

Fig. 2. Success probability, taking into account only intra-route interference, as a function of ρ, for $N = 10$ and $d = 1, 2, 3, 4$. The lower-bound calculated in Proposition 2 becomes tighter as d increases. ($b = 3$, $\theta = 6$ dB, $p = 0.1$)

TABLE II
MAIN ASSUMPTIONS OF SECTION II

Assumption	Comments
Inter-route interference: PPP and iid across time	Crucial; reasonable for small MA probabilities (see Fig. 9)
Hop success probabilities: equal to success probability of "worst" hop	Conservative; can be relaxed, but would lead to cumbersome expressions; reasonable for range of interest of path-loss exponents (see Fig. 10)
Transmission events: independent	Crucial; reasonable for small MA probabilities (see Fig. 11)

IV. BACKLOGGED SOURCES

A. Evaluation of the mean end-to-end delay

We first determine the probability of transmission ρ when the source is backlogged.

Proposition 3 *If the source is backlogged and $p_o < p$, then $\rho = p_o$.*

Proof: Recall the analysis in [20]. Since packet successes are independent events with probability p_s, if $p_o p_s < p p_s$, packets arrive to the first (and all subsequent relays) with probability $p_o p_s$. Hence the probability that a relay has a non-empty queue is $p_o p_s/(p p_s) = p_o/p$, which yields $\rho = p_o/p \cdot p = p_o$ (same as the source). ∎

Setting $\rho = p_o$ in (12), we readily obtain p_s. Note that the condition $p_o < p$ is necessary for the stability of the relay queues, as it ensures that the packet arrival rate does not exceed the packet service rate. We now evaluate the mean end-to-end delay D, defined as the mean total time (in slots) that it takes a packet to travel to the destination from the moment of its first transmission attempt at the source.

Proposition 4 *If the source is backlogged, the end-to-end delay is given by*

$$D = \frac{d}{p_o p_s} + d(N-1)\frac{1-p_o p_s}{p_s(p-p_o)} - N(d-1). \tag{13}$$

Proof: Since a departure occurs from the source every d slots independently with probability $p_o p_s$, the mean service time measured from the first transmission attempt till the packet is successfully received by the first relay, is $H_s = d/(p_o p_s) - d + 1$. For $p_o < p$, packets arrive at a relay every d slots with probability $p_o p_s$ and are serviced with probability $p p_s$. The mean service time for the head-of-line (HOL) packet at a relay is therefore $H_r = d/(p p_s) - d + 1$. The mean waiting time at a relay, W_r, defined as the mean total time from the moment a packet arrives at the end of the queue till it becomes the HOL packet, is calculated with standard queueing theory. The probability that there are k packets in the queue is

$$\pi_k = \frac{(p_o/p)^k}{1 - p_o p_s} \left(\frac{1 - p p_s}{1 - p_o p_s} \right)^{k-1} (1 - p_o/p), \quad k \geq 1. \quad (14)$$

By Little's theorem, W_r is the average queue size, excluding the HOL packet, divided by the arrival rate, in this case $p_o p_s / d$. Using (14), we find that

$$W_r = \frac{d}{p_o p_s} \sum_{k=2}^{\infty} (k-1)\pi_k = d \frac{p_o}{p} \frac{1 - p p_s}{p_s (p - p_o)}. \quad (15)$$

By definition, $D = H_s + (N-1)(H_r + W_r)$, and (13) follows. ∎

Remarks on Proposition 4: Since a packet is received by the destination every d slots with probability $p_o p_s$, the first term in (13) is the inverse of the end-to-end throughput $T = p_o p_s / d$. The second term is the mean total time from the moment a packet arrives at the end of the queue of the first relay till it arrives at the destination. It is proportional to $(p_s(p - p_o))^{-1}$, i.e., the inverse of the difference between the packet service and arrival rates at each relay buffer. Hence, if $N > 1$, a necessary condition for finite D is $p_o < p$.

From (13), the following upper bound can be readily obtained, which is tight for "small" p.

Corollary 1 *If the source is backlogged, $D \lesssim \bar{D}$, where*

$$\bar{D} = \frac{d}{p_o p_s} + \frac{d(N-1)}{(p - p_o) p_s}. \quad (16)$$

The bound is tight for $p \to 0$.

In the next section, we pursue the optimization of $\bar{D}$ over the parameters N, d, p_o for the cases of extrinsic and intrinsic interference. We obtain two kinds of results: (a) Exact expressions or tight bounds on the delay-optimal value of each parameter, keeping the other parameters fixed, and (b) asymptotic expressions for the jointly delay-optimal parameter values, as $\lambda_{\text{ex}} \to \infty$ for extrinsic interference, and $\lambda \to \infty$ for intrinsic interference. Note that, in an interference-limited network, (12) depends only on the product $\lambda_{\text{ex}} c R^2$ for extrinsic interference and $\lambda c R^2$ for intrinsic interference. Hence, all asymptotic results may equivalently be derived letting $\lambda_{\text{ex}} c R^2 \to \infty$ and $\lambda c R^2 \to \infty$, respectively. The delay-optimal parameter values and the respective delay and throughput are denoted by the superscript "*"[3]. For analytical tractability, we relax the integer constraints on N and d and let $N \in [1, +\infty)$, $d \in [1, N]$.

We close this section by suggesting how the framework presented in this paper can also be employed to compute the delay in a network where the distance R of each source-destination pair is drawn in an iid fashion from a given distribution. For each R, we let $N(R) = R/r$, where r is an inter-relay distance r that does not depend on R. Therefore, on average, the number of hops performed in the network is $\mathbb{E}[R]/r$, where the expectation is taken with respect to the distribution of R. The relevant interferer density is $\lambda_{\text{PPP}} = \lambda p_o \mathbb{E}[R]/(rd)$, and the mean delay in the network can readily be computed by (13), where the optimization parameters are now r, d, p_o, with $\mathbb{E}[R]$ in place of the common distance R of the homogeneous setting.

B. Extrinsic interference

We consider the cases of no intra-route spatial reuse ($d = N$) and intra-route spatial reuse ($d < N$) separately.

1) No intra-route spatial reuse ($d = N$): In the following proposition, the delay-optimal N, p_o are determined.

Proposition 5 *Let $\lambda_{\text{PPP}} = \lambda_{\text{ex}}$ and $d = N$.*

- *If $\lambda_{\text{ex}} c R^2 > 1$, then, for given p_o,*

$$N^* \in \begin{cases} \left[\sqrt{\lambda_{\text{ex}} c} R, \sqrt{2\lambda_{\text{ex}} c} R \right) & p_o \in (0, p/2], \\ \left[1, \sqrt{\lambda_{\text{ex}} c} R \right) & p_o \in (p/2, p). \end{cases} \quad (17)$$

- *For given $N > 1$*

$$p_o^* = \frac{p}{1 + \sqrt{N - 1}}. \quad (18)$$

Proof: See Appendix A. ∎

Remarks on Proposition 5:

1. For given λ_{ex}, in the light-traffic regime, i.e., $p_o \to 0$, $\bar{D} \approx 1/T$, so $N^* \to \sqrt{2\lambda_{\text{ex}} c} R$, which is the value of N that maximizes the end-to-end throughput $T = p_o p_s / N = p_o \mathrm{e}^{-\lambda_{\text{ex}} c (R/N)^2} / N$. As we move into the high-traffic regime, i.e., $p_o > p/2$, the second term of (16), which increases with N^2, dominates the delay. Therefore, a smaller number of hops is more delay-efficient and $N^* < \sqrt{\lambda_{\text{ex}} c} R$.
2. The delay-optimal p_o decreases as $\Theta(1/\sqrt{N})$. For a given N, (18) achieves the best tradeoff between throughput and total time spent in the relay queues.

We now determine the jointly delay-optimal (N, p_o) as $\lambda_{\text{ex}} \to \infty$.

Proposition 6 *Let $\lambda_{\text{PPP}} = \lambda_{\text{ex}}$ and $d = N$. The jointly delay-optimal (N, p_o) for $\lambda_{\text{ex}} \to \infty$ are*

$$N^* \sim \sqrt{\lambda_{\text{ex}} c} R \quad (19)$$

$$p_o^* \sim \frac{p}{(\lambda_{\text{ex}} c R^2)^{1/4}}. \quad (20)$$

The respective minimum delay is

$$\bar{D}^* \sim \frac{\lambda_{\text{ex}} c R^2 \mathrm{e}}{p} \left(1 + \frac{2}{(\lambda_{\text{ex}} c R^2)^{1/4}} \right). \quad (21)$$

Proof: See Appendix B. ∎

[3]We do not employ different notation for the optimal and jointly-optimal parameter values. To make the distinction clear, we state when the parameters are separately or jointly optimized.

Remarks on Proposition 6:
1. From (21), it is seen that $\bar{D}^* = \Theta(\lambda_{\rm ex})$. The linear scaling is due to the factor N^2 in (16) and the fact that $N^* = \Theta(\sqrt{\lambda_{\rm ex}})$. Intuitively, a HOL packet has to wait at least N slots before a retransmission attempt, and there are N buffers in the route. The respective delay-optimal throughput is $T^* = \Theta(p_o^*/N^*) = \Theta(\lambda_{\rm ex}^{-3/4})$.
2. The *throughput-optimal* strategy for all $\lambda_{\rm ex}$ is to set $N = \sqrt{2\lambda_{\rm ex}c}R$ (see remark on Proposition 5) and $p_o = p$ (if $p_o = p$ the delay is infinite, though). So, asymptotically, the throughput-optimal number of hops is larger than the delay-optimal number of hops by a factor $\sqrt{2}$. The resulting maximum throughput is $T = \Theta(1/\sqrt{\lambda_{\rm ex}})$. Hence, a throughput penalty of $\Theta(\lambda_{\rm ex}^{1/4})$ is incurred by the delay-optimal policy due to the fact that $p_o^* = \Theta(\lambda_{\rm ex}^{-1/4})$.

2) With intra-route spatial reuse ($d < N$): Given the inefficiency of a protocol which allows only one node to be scheduled at a time, we now let $d < N$. In the following proposition, we determine the delay-optimal N, p_o.

Proposition 7 *Let $\lambda_{\rm PPP} = \lambda_{\rm ex}$ and $d \in [1, N)$.*

- *If $2\lambda_{\rm ex}cR^2 > 1$, then, for given p_o,*

$$N^* \in \begin{cases} \left[\sqrt{2\lambda_{\rm ex}c}R, \sqrt{2(p/p_o)\lambda_{\rm ex}c}R\right) & p_o \in (0, p/2], \\ \left[1, \sqrt{2\lambda_{\rm ex}c}R\right) & p_o \in (p/2, p). \end{cases} \tag{22}$$

- *For given N, d*

$$p_o^* \lesssim \frac{2}{\sqrt{\delta^2 + 4(N-1)p^{-1}(\delta + p^{-1})} + \delta}. \tag{23}$$

The bound is tight for $N \to \infty$.

Proof: See Appendix C. ∎

Remarks on Proposition 7: For given $\lambda_{\rm ex}$, if $p_o \to 0$, the upper bound in (22) goes to infinity. Indeed, for $p_o \to 0$, $N^* \to \infty$ is delay-optimal, since $\bar{D}$ (see (45) in proof) is dominated by $1/T$, where $T = p{\rm e}^{-\lambda_{\rm ex}c(R/N)^2 - \delta p_o}/d$, and setting $N^* \to \infty$ maximizes T. Also, note that N^* does not depend on d, which is easy to see from (45). In contrast, p_o^* in (23) is a decreasing function of δ (i.e., an increasing function of d), as well as N.

Based on Proposition 7, we now derive the jointly delay-optimal (N, d, p_o), as $\lambda_{\rm ex} \to \infty$.

Proposition 8 *Let $\lambda_{\rm PPP} = \lambda_{\rm ex}$ and $d \in [1, N)$. The jointly delay-optimal (N, p_o, d) for $\lambda_{\rm ex} \to \infty$ are $d^* \sim 1$ and*

$$N^* \sim \sqrt{2\lambda_{\rm ex}c}R \tag{24}$$

$$p_o^* \sim \frac{p}{\sqrt{(1+\delta(1)p)}(2\lambda_{\rm ex}cR^2)^{1/4}} \tag{25}$$

The respective minimum delay is

$$\bar{D}^* \sim \frac{\sqrt{2\lambda_{\rm ex}c}eR}{p}\left(1 + \frac{\sqrt{1+\delta(1)p}}{(2\lambda_{\rm ex}cR^2)^{1/4}}\right). \tag{26}$$

Proof: See Appendix D. ∎

Remarks on Proposition 8:
1. In the limit $\lambda_{\rm ex} \to \infty$, (slotted) ALOHA is the delay-optimal MAC protocol. The reason that maximum reuse minimizes the delay is that, p_o^* (as well as the busy probability of the relay buffers p_o^*/p) goes to zero when $\lambda_{\rm ex} \to \infty$. Hence, $p_{s,\rm i} = {\rm e}^{-\delta p_o} \to 1$, and $\bar{D}$ in (16) is proportional to d, making $d = 1$ the optimal choice. From (12), it is also seen that the optimal hop success probability is $p_s^* \sim {\rm e}^{-1/2}$.
2. N^* in (24) is larger than the respective one in (19) by a factor of $\sqrt{2}$. This is the price paid in terms of resources, i.e., relays, for allowing intra-route spatial reuse.
3. The minimum delay scales as $\bar{D}^* = \Theta(\sqrt{\lambda_{\rm ex}})$, i.e., there is a delay gain of $\Theta(\sqrt{\lambda_{\rm ex}})$ compared to the case of no reuse. Since $T = p_o p_s/d$, the respective delay-optimal throughput scales as $T^* = \Theta(\lambda_{\rm ex}^{-1/4})$, so the throughput gain is also $\Theta(\sqrt{\lambda_{\rm ex}})$.
4. The throughput-optimal strategy selects (N, d, p_o) to maximize $T = p_o{\rm e}^{-\lambda_{\rm ex}c(R/N)^2 - \delta p_o}/d$. It is clear that, for a given $\lambda_{\rm ex}$, $N \to \infty$ maximizes T, which reduces the problem to selecting (d, p_o) to maximize $p_o{\rm e}^{-\delta(d)p_o}/d$. Since the maximum throughput is a constant with respect to $\lambda_{\rm ex}$, the throughput penalty incurred by the delay-optimal policy is $\Theta(\lambda_{\rm ex}^{1/4})$, as in the case of no reuse.

C. Intrinsic interference

We now study the case of intrinsic interference, i.e., $\lambda_{\rm PPP} = \lambda N p_o/d$. For lack of space (and similarity of the relevant derivations), we only state the asymptotic results for $\lambda \to \infty$. As in the case of extrinsic interference, we consider $d = N$ and $d < N$ separately.

1) No intra-route spatial reuse ($d = N$): The interferer density is $\lambda_{\rm PPP} = \lambda N p_o/N = \lambda p_o$. The jointly delay-optimal (N, p_o) when $\lambda \to \infty$ are determined in the following proposition.

Proposition 9 *Let $\lambda_{\rm PPP} = \lambda p_o$ and $d = N$. The jointly delay-optimal (N, p_o) for $\lambda \to \infty$ are*

$$N^* \sim \left(\frac{\zeta\lambda cR^2 p}{2}\right)^{1/3} \tag{27}$$

$$p_o^* \sim \left(\frac{p^2}{4\zeta\lambda cR^2}\right)^{1/3}, \tag{28}$$

where ζ is a constant in $(1, 2)$. The minimum delay is

$$\bar{D}^* \sim {\rm e}^{1/\zeta}\left(\frac{\zeta\lambda cR^2}{2p}\right)^{1/3}\left(3\left(\frac{\zeta\lambda cR^2}{2}\right)^{1/3} - \frac{1}{p^{1/3}}\right). \tag{29}$$

Proof: See Appendix E. ∎

Remarks on Proposition 9:
1. The minimum delay scales as $\bar{D}^* = \Theta(\lambda^{2/3})$, and the respective delay-optimal throughput as $T^* = \Theta(\lambda^{-2/3})$. We can interpret this result by defining the delay and throughput exponents $\Delta = \lim_{\lambda\to\infty} \log \bar{D}(\lambda)/\log\lambda$ and $\tau = \lim_{\lambda\to\infty} \log T(\lambda)/\log\lambda$ and letting $p_o = \lambda^{-\kappa}$, where $\lambda > 1$. From (17), it is seen that, for a given p_o, the delay-optimal N must satisfy $N = \Theta(\sqrt{p_o(\lambda)\lambda}) = \Theta(\lambda^{\frac{1-\kappa}{2}})$. Substituting in (13), we have that $\Delta(\kappa) = \max\{(\kappa+1)/2, 1-\kappa\}$ and $\tau(\kappa) = -(\kappa+1)/2$. The value of κ that minimizes $\Delta(\kappa)$ is $1/3$, which yields $\Delta(1/3) = \tau(1/3) = 2/3$.
2. The constant ζ arises due to the fact that N^* is in the range $(\sqrt{\lambda c p_o^*}R, 2\sqrt{\lambda c p_o^*}R)$ (see proof).

TABLE III
SCALING LAWS FOR BACKLOGGED SOURCE, FOR THE CASES OF EXTRINSIC AND INTRINSIC INTERFERENCE.

	extrinsic: $\lambda_{\rm ex} \to \infty$		intrinsic: $\lambda \to \infty$	
Metric	$d = N$	$d < N$	$d = N$	$d < N$
$\bar{D}^*$	$\Theta(\lambda_{\rm ex})$	$\Theta(\sqrt{\lambda_{\rm ex}})$	$\Theta(\lambda^{2/3})$	$\Theta(\sqrt{\lambda})$
T^*	$\Theta(1/\sqrt{\lambda_{\rm ex}})$	$\Theta(1/\sqrt{\lambda_{\rm ex}})$	$\Theta(\lambda^{-2/3})$	$\Theta(1/\sqrt{\lambda})$
N^*	$\Theta(\sqrt{\lambda_{\rm ex}})$	$\Theta(\sqrt{\lambda_{\rm ex}})$	$\Theta(\lambda^{1/3})$	$\Theta(\sqrt{\lambda})$
d^*	-	~ 1	-	~ 1
p_o^*	$\Theta(\lambda_{\rm ex}^{-1/4})$	$\Theta(\lambda_{\rm ex}^{-1/4})$	$\Theta(\lambda^{-1/3})$	$\Theta(1/\sqrt{\lambda})$
p_s^*	$\Theta(1)$	$\Theta(1)$	$\Theta(1)$	$\Theta(1)$

3. The throughput $T = p{\rm e}^{-\lambda c p_o (R/N)^2}/N$ is maximized for $p_o = p$ and $N = \sqrt{2\lambda pcR}$. The maximum throughput scales as $T = \Theta(1/\sqrt{\lambda})$, hence the delay-optimal policy incurs a throughput penalty of $\Theta(\lambda^{1/6})$.

2) With intra-route spatial reuse ($d < N$): The interferer density is $\lambda_{\rm PPP} = \lambda N p_o/d$.

Proposition 10 *Let $\lambda_{\rm PPP} = \lambda N p_o/d$ and $d \in [1, N)$. The jointly delay-optimal (N, p_o, d) for $\lambda \to \infty$ are $d^* \sim 1$ and*

$$N^* \sim \sqrt{2\lambda cpR} \tag{30}$$

$$p_o^* \sim \sqrt{\frac{p}{2\lambda cR^2}}. \tag{31}$$

The respective minimum delay is

$$\bar{D}^* \sim 2\sqrt{\frac{2{\rm e}\lambda cR^2}{p}}. \tag{32}$$

Proof: See Appendix F. ∎

Remarks on Proposition 10:

1. As in the case of extrinsic interference, ALOHA is asymptotically delay-optimal. The minimum delay scales as $\bar{D}^* = \Theta(\sqrt{\lambda})$, i.e., there is a delay gain of $\Theta(\lambda^{1/6})$ compared to the case of no reuse (Proposition 9). Since $T = p_o p_s/d$, the respective delay-optimal throughput scales as $T^* = \Theta(1/\sqrt{\lambda})$, so the throughput gain is also $\Theta(\lambda^{1/6})$. These gains are achieved by increasing the number of hops from $N^* = \Theta(\lambda^{1/3})$, when $d = N$, to $N^* = \Theta(\sqrt{\lambda})$.

2. The throughput-optimal strategy selects (N, d, p_o) to maximize $T = p_o {\rm e}^{-\lambda c p_o R^2/(Nd) - \delta p_o}/d$. Since $N \to \infty$ maximizes T, the maximum throughput is a constant with respect to λ. Hence, the throughput penalty incurred by the delay-optimal policy is $\Theta(\sqrt{\lambda})$.

The scaling laws derived throughout Section IV are summarized in Table III. We now provide numerical results for specific values of the network parameters.

D. Numerical results

Let $R = 500$ m, $b = 3$, $\theta = 6$ dB and $p = 0.1$. In Fig. 3, D in (13) is plotted vs. $\lambda_{\rm ex}$ for the case of extrinsic interference, and λ for the case of intrinsic interference. D is numerically optimized over N and p_o when $d = N$ (no reuse) and $d = 1$ (maximum reuse, or slotted ALOHA). Fig. 4 shows the respective delay-optimal numbers of hops. The theoretical expressions for $\bar{D}^*$ and N^*, derived in this section, are also plotted for comparison. Note that, even though asymptotic, they provide good approximations of the respective minimum delay and delay-optimal number of hops for a realistic range of densities. Indicatively, for the case of intrinsic interference and $\lambda = 10^{-4}$ m^{-2}, Fig. 4 shows that 3 hops are required when no reuse is employed, while 9 hops are required with maximum reuse, when the source-destination distance is 500 m. It is also apparent that, for the selected parameter values, maximum reuse outperforms no reuse for all density values, but the required number of hops is larger. In the case of extrinsic interference, the ratio of the delay-optimal N for maximum reuse and no reuse is approximately $\sqrt{2}$, while, for intrinsic interference, this ratio increases as $\lambda^{1/6}$. These observations are in agreement with the scaling laws listed in Table III.

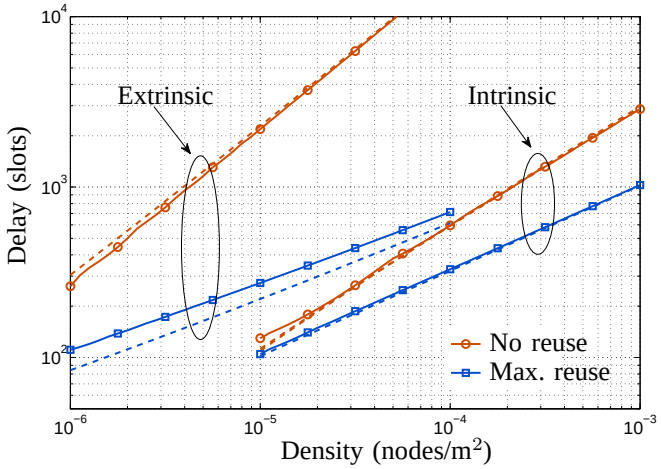

Fig. 3. D in (13) plotted in solid lines vs. $\lambda_{\rm ex}$ for extrinsic interference, and λ for intrinsic interference. Maximum reuse ($d = 1$) corresponds to a slotted ALOHA MAC. For each density, D is numerically optimized over N and p_o. The expressions for $\bar{D}^*$ given, from left to right, in (21), (26), (29) and (32) are also plotted for comparison (dashed). ($R = 500$ m, $p = 0.1$, $b = 3$, $\theta = 6$ dB)

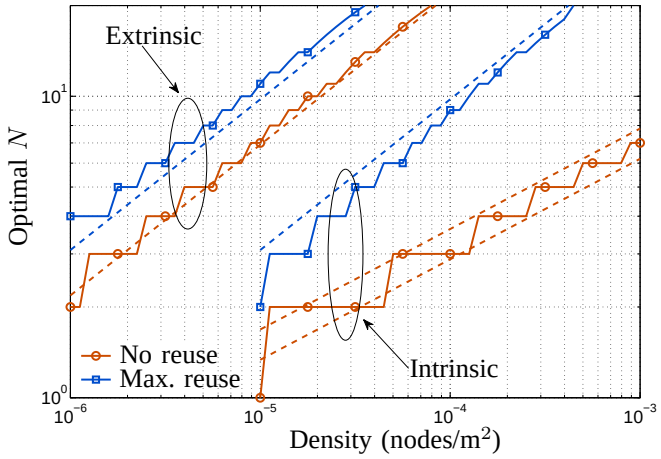

Fig. 4. Delay-optimal N, corresponding to Fig. 3. The solid lines (staircase curves) correspond to the delay-optimal N found numerically. The dashed lines correspond, from left to right, to (19), (24), (27) and (30). For extrinsic interference, the ratio of the delay-optimal N for maximum reuse and no reuse is $\sqrt{2}$; for intrinsic interference, this ratio increases as $\lambda^{1/6}$ ($R = 500$ m, $p = 0.1$, $b = 3$, $\theta = 6$ dB)

V. Geometric arrivals

In the previous section we examined in detail a heavy-traffic scenario, where the source always has packets to transmit. In this section, we briefly treat the case of geometric arrivals at the source. The analysis follows closely the one of Section IV. We focus on the case of intrinsic interference, i.e., $\lambda_{\rm PPP} = \lambda N\rho/d$, and $p_o = p$ (the cases of extrinsic interference or $p_o \neq p$ can be treated very similarly).

The main result is stated in the following proposition. Let $\mathcal{W}(x),\ x \geq -{\rm e}^{-1}$, denote the principal branch of the Lambert function [25].

Proposition 11 *Assume that a new packet arrives at the source every d slots with probability a and interference is intrinsic. If $a < p\exp(-\gamma p)$, where $\gamma = \lambda c R^2/(Nd) + \delta$, then*

$$p_s = \exp\left(\mathcal{W}(-a\gamma)\right) \tag{33}$$

and

$$\rho = a\exp\left(-\mathcal{W}(-a\gamma)\right). \tag{34}$$

The mean end-to-end delay D, measured from the moment a packet arrives at the end of the source queue, is $D = \bar{D} - N(d-1)$, where

$$\bar{D} = Nd\frac{1-a}{pp_s - a}. \tag{35}$$

Proof: The condition $a < p\exp(-\gamma p)$ ensures that the queues are stable — see [26, Prop. 1]. In this case, the packet arrival probability to each relay is a. Hence, the probability that a node is a transmitter is $\rho = (a/pp_s)\cdot p = a/p_s$. From (12), this results in the following fixed-point equation over p_s

$$p_s = \exp\left(-\gamma\frac{a}{p_s}\right). \tag{36}$$

Eq. (36) has two solutions if and only if $a < (\gamma{\rm e})^{-1}$, which always holds if $a < p\exp(-\gamma p)$. The smaller solution is increasing in a, on the basis of which it is rejected, since it represents a network where the hop success probability increases with increasing traffic. Rewriting (36) as $-a\gamma/p_s\exp\left(-a\gamma/p_s\right) = -a\gamma$ and applying the Lambert function to both sides, we obtain (33). Since $\rho = a/p_s$, (34) follows.

The proof of (35) follows the one of Proposition 4. If $a < pp_s$, the packet arrival probability to all nodes is a and the packet service probability is pp_s. Due to symmetry, $D = N(H+W)$, where $H = d/(pp_s) - d + 1$ and

$$W = d\frac{a}{pp_s}\frac{1-pp_s}{pp_s - a}, \tag{37}$$

and (35) follows. ∎

Remarks on Proposition 11:

1. p_s is a decreasing function of a. In the extreme case $a = 0$, the throughput is zero and $p_s = 1$.
2. The fixed-point equation (36) is the result of the assumption that packet successes are iid. Note that similar "decoupling" assumptions employed in [27] and [28] also resulted in fixed-point equations for the transmission probability.
3. If the queues are stable, the end-to-end throughput is $T = a/d$, since a packet arrives at the destination every d slots with probability a. For a given end-to-end throughput requirement $T = T_o$, we can show that the number of hops N^* that minimizes (35) satisfies the relation

$$N^* = \frac{\lambda c R^2 p T_o}{\left(1+\mathcal{W}(-\gamma^* dT_o)\right)\left(p{\rm e}^{\mathcal{W}(-\gamma^* dT_o)} - dT_o\right)}, \tag{38}$$

where $\gamma^* = \lambda c R^2/(N^* d) + \delta$. It follows that $N^* = \Theta(\lambda T_o)$ and $\bar{D}^* = \Theta(\lambda T_o)$. This is a manifestation of the scaling law derived in [3], in the context of our model, which assumes perfectly placed relays and interferers located according to a PPP.

VI. Application

A. Simulated network setting

In the previous sections, we developed an analytical framework to evaluate and optimize the mean total delay from the source to the destination in the presence of interferers that form a PPP. In particular, the case of intrinsic interference was considered, in order to evaluate the delay in a network with mutually interfering routes. We now examine how the results of Section IV can be applied in a setting where backlogged sources have to route packets to their destinations by employing a common pool of relays. We consider a network where *both* the source and relay locations are drawn from a PPP Π_t of total density λ_t, and a node is a source with probability μ, or a relay with probability $1-\mu$. Therefore, sources and relays form two independent PPPs, Π_s and Π_r, with densities $\lambda = \mu\lambda_t$ and $\lambda_r = (1-\mu)\lambda_t$, respectively. Each source has a destination at distance R and random orientation, and selects out of the available relays the ones which are closest to the delay-optimal locations. In each route formed in this manner, the nodes observe the MAC protocol described in Section II, in a slot-synchronous manner[4].

The simulated network departs from the theoretical model as relays are not perfectly placed on the line between the source and destination, and two or more routes may utilize the same relay. We first discuss the impact of these factors on the theoretical performance, and then describe our simulation campaign and results.

B. Imperfect relay placements

For ease of exposition, we consider $N > 2$, and no reuse, i.e., $d = N$. Assume that the second relay selected is displaced by x from the ideal position on the source-destination line, where $x < r$ and $r = R/N$ is the hopping distance. We derive the incurred delay penalty for small perturbations $x \ll r$.

Proposition 12 *Let $x \ll r = R/N$, $x > 0$, $N > 2$, be the displacement of the second relay from the ideal position. When $x \to 0$, the delay increase $\delta\bar{D} = \bar{D}_{\rm disp} - \bar{D}$ is given by*

$$\delta\bar{D} = \frac{4N\lambda c p_o p{\rm e}^{\lambda c p_o r^2}}{(p-p_o)^2}\left(1 + 2\lambda c p_o r^2\frac{p+p_o}{p-p_o}\right)x^2 + O(x^4), \tag{39}$$

[4]The slot boundaries are synchronized, but not the TDMA schedules, i.e., $\mathcal{P}(t)$ (see Section II) is generally different across routes in a given slot t.

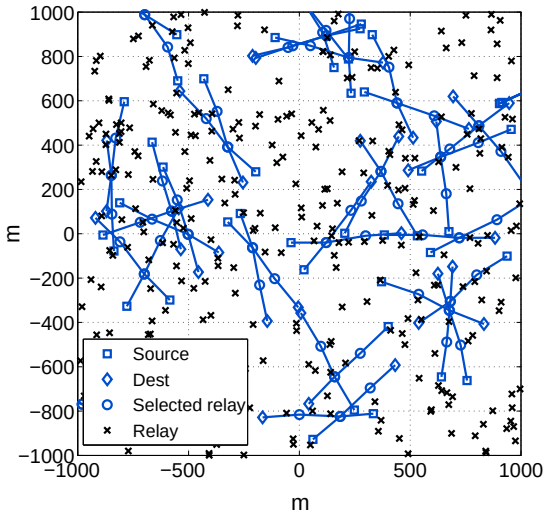

Fig. 5. Crossings of different source-destination pairs at common relays for a network with $\lambda = 10^{-4}$ m^2, $N = 3$, $R = 500$ m and a relay density $\lambda_r = 32\lambda$. Utilized (non-utilized) relays are shown with circles (crosses).

where $\bar{D}$ is defined in (16).

Proof: From (16), $\delta\bar{D}$ is found to be

$$\delta\bar{D} = \frac{N\mathrm{e}^{\lambda c p_o r^2}}{p\mathrm{e}^{-\lambda c p_o (x^2+2crx)}} + \frac{N\mathrm{e}^{\lambda c p_o r^2}}{p\mathrm{e}^{-\lambda c p_o (x^2-2crx)}} - \frac{2N\mathrm{e}^{\lambda c p_o r^2}}{p - p_o}.$$

Taking the Taylor series expansion at $x = 0$, we obtain (39). ∎

Remarks on Proposition 12: Eq. (39) implies that the delay penalty due to imperfect relay placement is more severe if $p_o \to p$, i.e., if the system is operated close to capacity, and it is proportional to N, if no intra-route reuse is employed. Moreover, for $x \ll R/N$, the penalty is approximately proportional to x^2 (and an even function of x, due to symmetry). If we set $x = (2\sqrt{\lambda_r})^{-1}$, which is the expected distance of the closest relay to the desired point, it follows that the delay penalty is also roughly inversely proportional to the density of relays in the network.

C. Route crossings

Each source selects the relays which are closest to the desired locations on the source-destination line. As shown in the example of Fig. 5, this results in the utilization of particular relays by more than one source-destination pair. If C is the number of times the typical relay node is actually employed as a relay in a network where the desired number of hops is N, we define the *crossing probability* $P_{\mathrm{cr},N} = \mathbb{P}(C > 1 | C > 0)$. The exact evaluation of $P_{\mathrm{cr},N}$ appears complicated, hence we resort to the following approximation. Let x be the typical relay in Π_r. Denote the point process of ideal relay locations as $\Pi_{r,\mathrm{ideal}}$, and let z be the closest point of $\Pi_{r,\mathrm{ideal}}$ to x, and z' the second closest. We define as $P'_{\mathrm{cr},2}$, the probability that, in a two-hop system (i.e., one ideal relay location per source-destination pair), x is the closest neighbor of Π_r to z', given that it is also the closest neighbor to z. Mathematically,

$$P'_{\mathrm{cr},2} = \mathbb{P}\left(\arg\min_{x' \in \Pi_r} |x' - z'| = x \;\middle|\; \arg\min_{x' \in \Pi_r} |x' - z| = x \right).$$

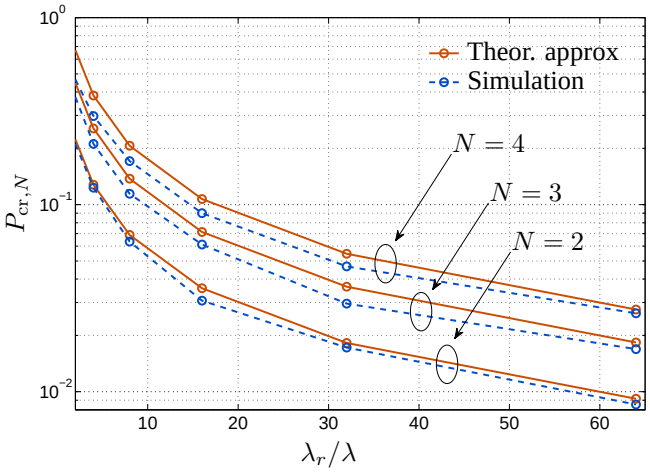

Fig. 6. Crossing probability vs. λ_r/λ for $N = 2, 3, 4$. The simulation results were obtained for $\lambda = 10^{-4}$ sources/m^2 and $R = 500$ m. The theoretical approximation in (40) is plotted for comparison.

For $N \geq 2$, we then approximate $P_{\mathrm{cr},N}$ by

$$P'_{\mathrm{cr},N} = (N-1)P'_{\mathrm{cr},2}, \tag{40}$$

since, for a sufficiently large relay density, (a) a relay is likely to be utilized by its neighboring points in $\Pi_{r,\mathrm{ideal}}$, and (b) the probability of a crossing should increase roughly proportionally with the desired number of hops. In the following proposition, we derive an expression for $P'_{\mathrm{cr},2}$.

Proposition 13 *$P'_{\mathrm{cr},2}$ is given by*

$$P'_{\mathrm{cr},2} = \frac{4/\pi}{1 + \frac{\lambda_r}{\lambda}} \int_0^{+\infty} \mathrm{d}t_1 \int_{t_1}^{+\infty} \mathrm{d}t_2 \int_0^{\pi} \mathrm{d}\theta \cdot t_1 t_2 \mathrm{e}^{-t_2^2 - \frac{\lambda_r}{\lambda\pi}\left(t_1^2(\pi-\phi) + t_2^2(\phi+\theta) + y t_1 \sin\phi\right)} \tag{41}$$

$$y = \sqrt{t_1^2 + t_2^2 - 2t_1 t_2 \cos\theta}$$

$$\phi = \tan^{-1}\left(\frac{t_2 \sin\theta}{t_1 - t_2\cos\theta}\right).$$

Proof: See Appendix G. ∎

$P_{\mathrm{cr},N}$ was evaluated by simulation over different relay densities and network realizations, for $N = 2, 3, 4$ hops, $\lambda = 10^{-4}$ sources/m^2 and $R = 500$ m. The results are plotted in Fig. 6, as a function of the ratio λ_r/λ. Is is seen that $P'_{\mathrm{cr},N}$ in (40), provides a good approximation of $P_{\mathrm{cr},N}$. We can verify that $P_{\mathrm{cr},N}$ roughly follows the trend $(N-1)(1 + 2\lambda_r/\lambda)^{-1}$.

D. Simulation results

We let $\lambda = 10^{-4}$ m^{-2}, $p = 0.1$, $b = 3$, $\theta = 6$ dB and perform a number of simulations for different values of N, d, R, p_o and λ_r. The network area is square, with size such that, on average, 2000 sources are included; for $\lambda = 10^{-4}$ m^{-2}, this corresponds to a square side of ≈ 4.5 km. For each operating point, we generate *one* network topology and run an experiment with duration 100000 slots (at the beginning of each experiment the node buffers are empty). In order to resolve conflicts when a relay is selected by more than one sources, packets with different destinations are stored in

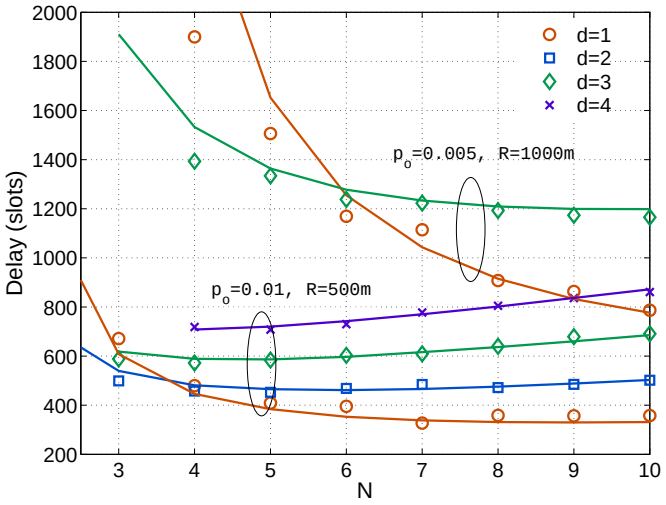

Fig. 7. Delay vs. number of hops for ($p_o = 0.01$, $R = 500$ m) and ($p_o = 0.005$, $R = 1000$ m), and various reuse factors. The markers correspond to simulation results obtained for $\lambda_r = 4N\lambda$ for each N and the solid curves correspond to (13).

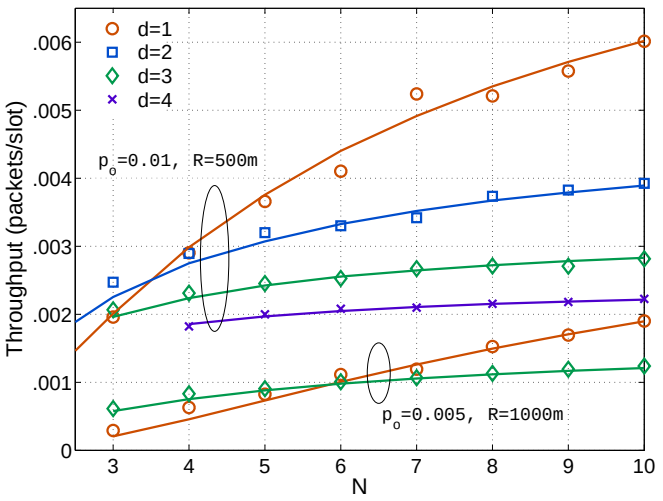

Fig. 8. Throughput vs. number of hops corresponding to Fig. 7.

a common queue and the following rule is applied at any given slot: if the relay is a receiver for one route and a transmitter for another, the reception fails; in all other cases, successful reception follows the SINR criterion (1). In order to avoid edge effects, for each topology, sample-metrics are only collected for the routes with the 200 innermost sources. For each operating point, the plotted metrics are obtained by averaging over routes (where applicable) and time slots.

We first select a relay density of $\lambda_r = 4N\lambda$, where N is the desired number of hops, such that, for a given number of hops, relays are found close to the desired locations with high probability. We consider two scenarios: $R = 500$ m and $R = 1000$ m, which are 10 and 20 times the expected closest-neighbor distance in the source PPP, i.e., $1/(2\sqrt{\lambda}) = 50$ m, respectively. According to (30) and (31), the corresponding optimal values of (N, p_o) are $(10, 0.01)$ and $(20, 0.005)$. Since the relay MA probability is set to $p = 0.1$, these values of p_o correspond to a traffic generation rate at 10% and 5% of capacity, respectively (Proposition 3).

In Figs. 7-8, we have plotted the theoretically computed delay (13) and throughput ($T = p_o p_s/d$), along with the simulation results, for N ranging from 3 to 10 hops, and various reuse factors. Figs 7-8 illustrate the general agreement between theory and simulation; the discrepancy is largest for small numbers of hops and reuse factors. The main message is that $d = 1$ (maximum reuse) is optimal once N is sufficiently large; for small N, it is more advantageous to space out transmissions by imposing a $d > 1$, e.g., for $p_o = 0.01$ and $R = 500$ m, $d = 2$ yields a smaller delay than $d = 1$ for $N < 4$, while for $p_o = 0.005$ and $R = 1000$ m, $d = 3$ yields a smaller delay than $d = 1$ for $N < 6$. In addition, note from Fig. 8 that, while there exists a delay-optimal number of hops, the throughput increases with N since the distance per hop decreases for fixed R.

The agreement between theoretical and simulation results in Figs. 7-8 implicitly demonstrates that the theoretical approach is valid in the considered regime. In Figs. 9-11, we look more closely at the assumptions that underly our analysis, which are listed in Table II. In order to validate the iid component of the first assumption[5], in Fig. 9 we select $N = 4$ and $d = 1, \ldots, 4$, and plot: the squares of the cdfs of the simulated interference power at the origin at odd and even time slots, $P_1(x) = \mathbb{P}(I_{n,o}(t) + I_{n,i}(t) \leq x)$ and $P_2(x) = \mathbb{P}(I_{n,o}(t+1) + I_{n,i}(t+1) \leq x)$; the simulated joint interference power cdf at the origin, over odd and even time slots, i.e., $P_{12}(x) = \mathbb{P}(I_{n,o}(t) + I_{n,i}(t) \leq x, I_{n,o}(t+1) + I_{n,i}(t+1) \leq x)$; and the product of the individual simulated cdfs, i.e., $P_1(x)P_2(x)$. The match between the curves is very good for the whole range of interference values and reuse factors, which implies that, in the considered regime, the temporal iid assumption is reasonable. This result also agrees with a recently discovered rule of thumb that the interference may be considered approximately temporally independent, if $p(1 - 2/b) < 0.1$ [29].

Fig. 10 shows the simulated success probabilities of the last hop and the worst-interfered hop, i.e., the hop with index $\lfloor \frac{1}{2} \lceil \frac{N}{d} \rceil \rfloor + 1$, that correspond to the set of curves ($p_o = 0.01$, $R = 500$ m) of Fig. 7. In almost all cases, the curve corresponding to the worst-interfered hop lies very slightly below the corresponding one for the last hop, indicating that the second assumption is also quite reasonable in the considered regime. Our interpretation of these results is that, while edge nodes suffer from less intra-route interference, the inter-route interference is the same (on average); for a path loss exponent $b = 3$, it dominates the total interference, such that edge effects can be safely neglected.

Fig. 11 is concerned with the last assumption of Table II. To this extent, we have plotted the simulated joint probability of transmission of two nodes in the same route at distance d hops, as well as the product of the respective individual probabilities of transmission. As in Fig. 10, the plotted curves correspond to the set of curves ($p_o = 0.01$, $R = 500$ m) of Fig. 7. The

[5]Since the source and relay locations form two independent PPPs, the interference power is generated from a PPP with very good approximation.

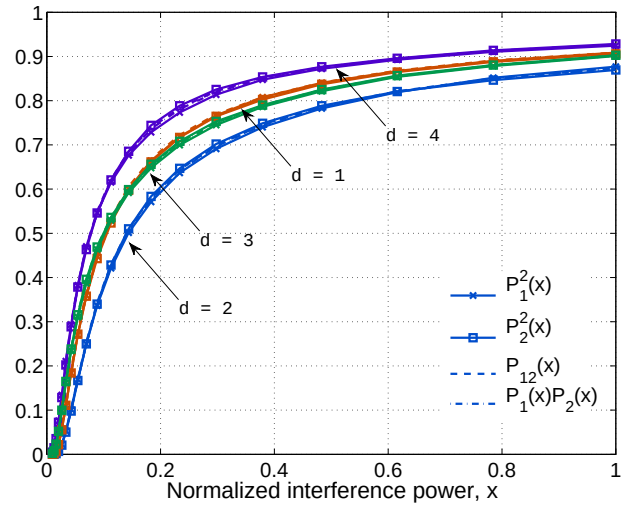

Fig. 9. Simulated interference power (at origin) cdfs for $N = 4$, $d = 1, \ldots, 4$ and ($p_o = 0.01$, $R = 500$ m). The x-axis is normalized to one. $P_1(x)$ and $P_2(x)$ are the interference power cdfs at odd and even time slots, and $P_{12}(x)$ is the joint interference power cdf over two consecutive slots. The conclusion is that the iid assumption is reasonable in the considered operation regime.

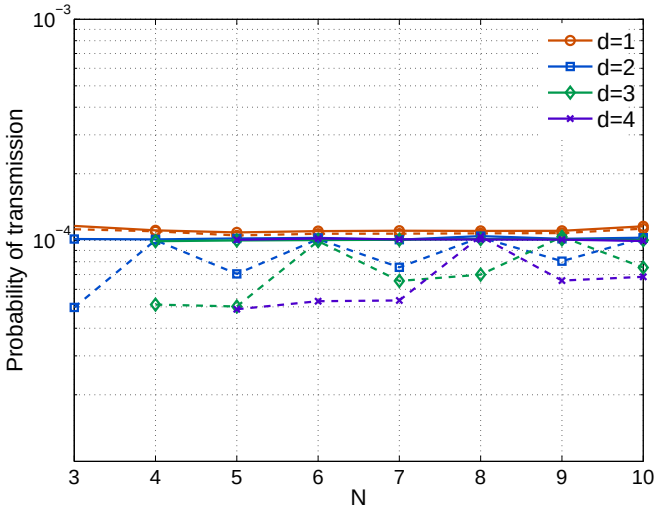

Fig. 11. Simulated joint probability that two nodes at distance d hops within a route are simultaneously transmitting (dashed line) and product of respective simulated individual probabilities of transmission (solid line), corresponding to the delay curves of Fig. 7 for ($p_o = 0.01$, $R = 500$ m). The maximum difference between the two curves is about 50% for all reuse factors.

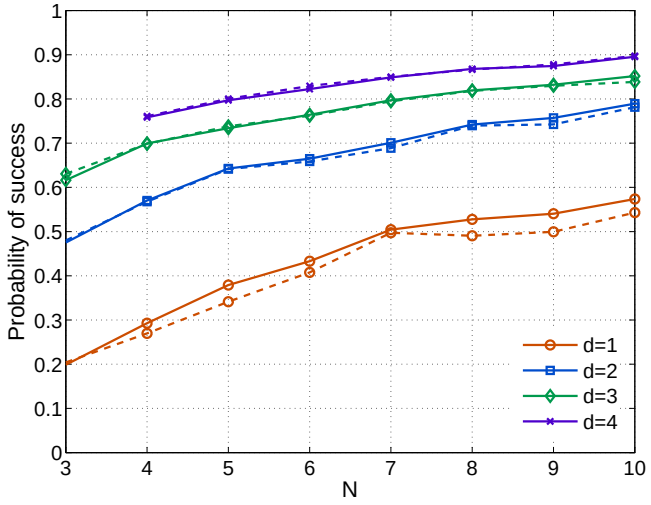

Fig. 10. Simulated success probabilities of last (solid line) and "worst" (dashed line) hops corresponding to the set of curves ($p_o = 0.01$, $R = 500$ m) of Fig. 7. The discrepancy is small due to the dominance of inter-route over intra-route interference for path-loss exponent $b = 3$.

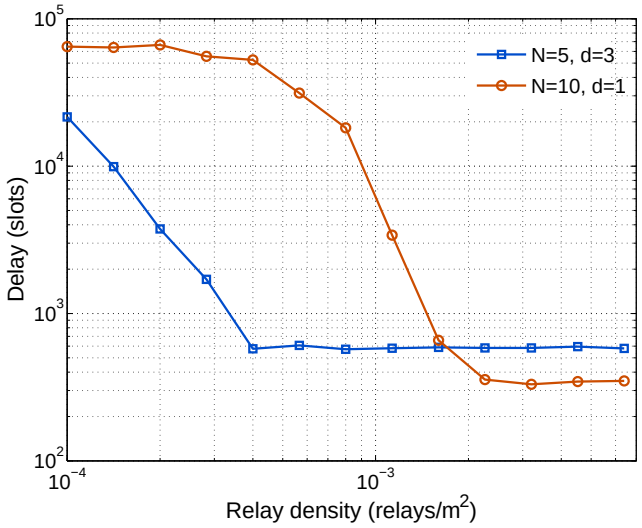

Fig. 12. Simulated delay vs. relay density for ($N = 5, d = 3$) and ($N = 10$, $d = 1$). The delay converges to the theoretically predicted value when $\lambda_r > N\lambda$. ($R = 500$ m, $p_o = 0.01$)

results indicate that the joint probability of transmission is smaller than the product by at most 50% for all considered values of N and d.

Finally, in Fig. 12, we examine the sensitivity of the delay with respect to the relay density. We select two operating points from those in Fig. 7: ($N = 5, d = 3$) and ($N = 10$, $d = 1$), and let the relay density λ_r vary between λ and 64λ (note that for these two points, the results in Fig. 7 were obtained for relay densities 20λ and 40λ, respectively). We observe that the simulated delay converges to the theoretically predicted value when λ_r takes values larger than $N\lambda$. Moreover, consistent with intuition, performing 10 hops (at maximum reuse) requires a larger relay density than 5 hops (at reuse factor 3) for convergence, as the attempted number of hops is larger. In particular, for $\lambda_r < 20\lambda$, the bottlenecks that occur at overutilized relays by multiple sources incur a significant delay penalty, and thus performing 5 instead of 10 hops results in smaller delay.

VII. Conclusions

We evaluated the end-to-end delay of multi-hop transmission in the presence of interferers that form a PPP, under a TDMA-ALOHA MAC protocol. We considered the case of an arbitrary interferer density, as well as the case where the density depends on the number of scheduled nodes per route and the transmission probability. The delay-optimal number of hops was determined, and asymptotic expressions were derived

for large values of the interferer density. Consistent with intuition, we obtained that, when the source is backlogged, a random access policy is asymptotically delay-optimal, but requires more hops than a TDMA-ALOHA protocol.

The theoretical results were applied to a delay-minimizing routing algorithm for networks with randomly distributed nodes. We simulated a static network setting, where both sources and relays formed a PPP, and each source performed the delay-optimal number of hops to its destination, by routing to the relays closest to the optimal locations. We confirmed that the main assumptions on which the analysis is based are reasonable for small enough MA probabilities; as a consequence, the match between the theoretical and simulated delay is also satisfactory in this regime. In addition, we assessed the sensitivity of the delay with respect to imperfect relay placements and relay-utilization by more than one source-destination pairs.

In conclusion, this paper combined elements from queueing theory and the theory of PPPs in order to obtain explicit end-to-end delay results for multi-hop networks with randomly placed nodes, fading and interference. These results fill in the gap between existing work on multi-hop networks, that has focused exclusively on scaling laws, and existing work on PPPs that has focused on throughput, without taking into account the effects of packet buffering.

ACKNOWLEDGMENTS

The partial support of the DARPA/IPTO IT-MANET program (grant W911NF-07-1-0028) and the U.S. National Science Foundation (grant CNS 10167423) is gratefully acknowledged.

APPENDIX

A. Proof of Proposition 5

Setting $d = N$ in (12) and (16)

$$\bar{D}(N, p_o) = N\left(\frac{1}{p_o} + \frac{N-1}{p-p_o}\right) \mathrm{e}^{\lambda_{\mathrm{ex}} c \left(\frac{R}{N}\right)^2}. \qquad (42)$$

The sign of $\partial\bar{D}/\partial N$ is determined by the function

$$f(N) = (p/p_o - 2)\left(N^2 - 2\lambda_{\mathrm{ex}} c R^2\right) + 2N(N^2 - \lambda_{\mathrm{ex}} c R^2).$$

We examine the two ranges of p_o separately:

- $p_o \in (0, p/2]$: If $p_o \in (0, p/2)$, $\partial\bar{D}/\partial N < 0$ for $N \leq \sqrt{\lambda_{\mathrm{ex}} c}R$ and $\partial\bar{D}/\partial N > 0$ for $N \geq \sqrt{2\lambda_{\mathrm{ex}} c}R$. If $p = p_o/2$, then $f(N) = 0$ yields $N^* = \sqrt{\lambda_{\mathrm{ex}} c}R$. This proves the first branch of (17).
- $p_o \in (p/2, p)$: We set $N = \sqrt{\alpha\lambda_{\mathrm{ex}} c}R$, $\alpha \geq 1$. Then

$$\begin{aligned} f(N)/(\lambda_{\mathrm{ex}} c R^2) = \\ 2\sqrt{\alpha\lambda_{\mathrm{ex}} c R^2}(\alpha - 1) + (p/p_o - 2)(\alpha - 2) > \\ 2\sqrt{\alpha\lambda_{\mathrm{ex}} c R^2}(\alpha - 1) - (\alpha - 2) > \\ 2\sqrt{\alpha}(\alpha - 1) - (\alpha - 2) > \\ (2\sqrt{\alpha} - 1)(\alpha - 1) \geq 0, \end{aligned}$$

  since $p/p_o > 1$, $\lambda_{\mathrm{ex}} c R^2 > 1$ and $\alpha \geq 1$. This proves the second branch of (17).

Finally, setting $\partial\bar{D}/\partial p_o|_{p_o = p_o^*} = 0$ yields (18).

B. Proof of Proposition 6

Substituting $p_o = p/(1 + \sqrt{N-1})$ in (42), we obtain

$$\bar{D} = Np^{-1}\left(1 + \sqrt{N-1}\right)^2 \mathrm{e}^{\lambda_{\mathrm{ex}} c \left(\frac{R}{N}\right)^2}. \qquad (43)$$

Setting $\partial\bar{D}/\partial N|_{N=N^*} = 0$

$$N^* + \frac{N^*(N^*-1)}{\sqrt{N^*-1}} - \frac{\lambda_{\mathrm{ex}} c R^2}{N^*}\left(1 + \frac{2\sqrt{N^*-1}}{N^*}\right) = 0. \qquad (44)$$

If $\lambda_{\mathrm{ex}} \to \infty$, (44) is satisfied only if $N^* \to \infty$. Letting $N^* \to \infty$, we obtain (19). Substituting (19) in (18) and (43), we obtain (20) and (21), respectively.

C. Proof of Proposition 7

From (12) and (16),

$$\bar{D}(N, d, p_o) = d\left(\frac{1}{p_o} + \frac{N-1}{p-p_o}\right) \mathrm{e}^{\lambda_{\mathrm{ex}} c \left(\frac{R}{N}\right)^2 + \delta p_o}. \qquad (45)$$

The sign of $\partial\bar{D}/\partial N$ is determined by the function

$$f(N) = N(N^2 - 2\lambda_{\mathrm{ex}} c R^2) - 2\lambda_{\mathrm{ex}} c R^2 (p/p_o - 2). \qquad (46)$$

We examine the two ranges of p_o separately:

- $p_o \in (p/2, p)$: $\partial D/\partial N > 0$, for $N \geq \sqrt{2\lambda_{\mathrm{ex}} c}R$, which proves the second branch of (22).
- $p_o \in (0, p/2]$: If $p_o \in (0, p/2)$, $\partial D/\partial N < 0$ for $N \leq \sqrt{2\lambda_{\mathrm{ex}} c}R$. If $p_o = p/2$, $\partial D/\partial N = 0$ yields $N^* = \sqrt{2\lambda_{\mathrm{ex}} c}R$. This proves the lower bound in the first branch of (22). In order to prove the upper bound, we set $N = \sqrt{2\alpha(p/p_o)\lambda_{\mathrm{ex}} c}R$, $\alpha \geq 1$. Then

$$\begin{aligned} f(N)/(\lambda_{\mathrm{ex}} c R^2) = \\ \sqrt{2\alpha(p/p_o)\lambda_{\mathrm{ex}} c}R\,(2\alpha p/p_o - 2) - 2(p/p_o - 2) > \\ 2\left(\sqrt{2}(p/p_o - 1) - (p/p_o - 2)\right) > \\ 2(\sqrt{2} - 1)(p/p_o - 1) > 0, \end{aligned}$$

  since $\alpha \geq 1$, $p/p_o > 2$ and $\lambda_{\mathrm{ex}} c R^2 > 1/2$. This concludes the proof of the upper bound.

For the proof of the second statement, we set

$$\left.\frac{\partial\bar{D}}{\partial p_o}\right|_{p_o = p_o^*} = -\frac{1}{p_o^{*2}} + \frac{\delta}{p_o^*} + \frac{N-1}{(p-p_o^*)^2} + \frac{(N-1)\delta}{p-p_o^*} = 0. \qquad (47)$$

This equation holds only if

$$-\frac{1}{p_o^{*2}} + \frac{\gamma}{p_o^*} < -\frac{N-1}{p^2} - \frac{(N-1)\delta}{p}. \qquad (48)$$

Solving over p_o^*,

$$(N-1)\left(\frac{1}{p^2} + \frac{\delta}{p}\right)(p_o^*)^2 + \delta p_o - 1 < 0,$$

which is equivalent to (23). For $N \to \infty$, $p_o^* \to 0$, therefore (48) becomes an equality. This proves the tightness of the bound.

D. Proof of Proposition 8

Assume that, for $\lambda_{\rm ex} \to \infty$, $N^* \to \infty$. Then, from (23), it follows that $p_o^* \sim p/\sqrt{N^*(1+\delta(d^*)p)}$. Setting (46) equal to zero at $N = N^*$ and substituting p_o^*, we obtain

$$(N^*)^3 - 2\lambda_{\rm ex} cR^2 N^* - 2\lambda_{\rm ex} cR^2 \left(\sqrt{N^*(1+\delta(d^*)p)} - 2\right) \sim 0,$$

or $N^* \sim \sqrt{2\lambda_{\rm ex} c}R$. Finally, substituting N^* and p_o^* in (45)

$$\bar{D}^* \sim d^* p^{-1} \left(\sqrt{N^*(1+\delta(d^*)p)} + N^*\right) \sqrt{\rm e},$$

Hence $d^* \sim 1$ and (26) follows.

We now return to the assumption that $N^* \to \infty$ for $\lambda_{\rm ex} \to \infty$. If $N^* = \Theta(1)$ for $\lambda_{\rm ex} \to \infty$, then (45) implies that $\bar{D}^* = {\rm e}^{\Theta(\lambda_{\rm ex})}$. Therefore, $N^* = \Theta(1)$ is rejected, and the proof is concluded.

E. Proof of Proposition 9

Setting $\lambda = \lambda p_o$ and $d = N$ in (12) and (13), we obtain that $p_s = {\rm e}^{-\lambda c p_o (R/N)^2}$ and

$$\bar{D}(N, p_o) = N \left(\frac{1}{p_o} + \frac{N-1}{p - p_o}\right) {\rm e}^{\lambda c p_o \left(\frac{R}{N}\right)^2}. \tag{49}$$

The jointly optimal (N^*, p_o^*) are found by solving the system $\partial \bar{D}/\partial N = 0$ and $\partial \bar{D}/\partial p_o = 0$. After some manipulations, we obtain

$$\frac{\lambda c R^2}{(N^*)^2}\left(\frac{1}{p_o^*} + \frac{N^*-1}{p - p_o^*}\right) = \frac{1}{(p_o^*)^2} - \frac{N^*-1}{(p-p_o^*)^2},$$
$$\frac{\lambda c R^2}{(N^*)^2}\left(\frac{1}{p_o^*} + \frac{N^*-1}{p - p_o^*}\right) = \frac{1}{2p_o^*}\left(\frac{1}{p_o^*} + \frac{2N^*-1}{p-p_o^*}\right).$$

Equating the right-hand sides

$$\frac{2N^*-1}{p/p_o^* - 1} + \frac{2N^*-2}{(p/p_o^* - 1)^2} = 1. \tag{50}$$

For $\lambda \to \infty$, we either have $p_o^* = \Theta(1)$ or $p_o^* \to 0$:

- If $p_o^* = \Theta(1)$, (50) demands that $N^* = \Theta(1)$. From (49), this implies that $\bar{D}^* = {\rm e}^{\Theta(\lambda)}$.
- If $p_o^* \to 0$, then, from (50), it is necessary that $N^* \to \infty$, which also implies that $p_o^* \sim p/(2N^*)$. Moreover, using the same steps as in the proof of Proposition 5, we can show that, since $p_o^* < p/2$, it is necessary that $N^* = \sqrt{\alpha \lambda p_o^* c}R$, where $\alpha \in (1,2)$. Setting $N^* = \sqrt{\alpha \lambda p_o^* c}R$ in $p_o^* \sim p/(2N^*)$, we obtain (27) and (28). Substituting (27) and (28) in (49) results in (29). Since, in this case, $\bar{D}^* = \Theta(\lambda^{2/3})$, the case $p_o^* = \Theta(1)$ is rejected, which concludes the proof.

F. Proof of Proposition 10

Setting $\lambda_{\rm PPP} = \lambda N p_o/d$ in (12) and (16), we obtain

$$\bar{D}(N, d, p_o) = d\left(\frac{1}{p_o} + \frac{N-1}{p-p_o}\right) {\rm e}^{\left(\frac{\lambda c R^2}{Nd} + \delta\right) p_o}. \tag{51}$$

Setting $\partial \bar{D}/\partial p_o = 0$ and $\partial \bar{D}/\partial N = 0$ at $(N, d, p_o) = (N^*, d^*, p_o^*)$, we have

$$\frac{1}{(p_o^*)^2} - \frac{N^*-1}{(p-p_o^*)^2} - \delta(d^*)K = \frac{\lambda c R^2}{N^* d^*}K, \tag{52}$$
$$\frac{N^*}{p_o^*(p-p_o^*)} = \frac{\lambda c R^2}{N^* d^*}K,$$

where $K \triangleq \left(\frac{1}{p_o^*} + \frac{N^*-1}{p-p_o^*}\right)$. Equating the right-hand sides and rearranging terms

$$\frac{N^*}{p_o^*(p-p_o^*)} + \frac{N^*-1}{(p-p_o^*)^2} + \frac{\delta(d^*)(N^*-1)}{p-p_o^*} = \frac{1}{(p_o^*)^2} - \frac{\delta(d^*)}{p_o^*}. \tag{53}$$

For $\lambda \to \infty$, we either have $p_o^* = \Theta(1)$ or $p_o^* \to 0$:

- If $p_o^* \to 0$, then (53) yields
$$N^* p_o^* + (N^*-1)(p_o^*)^2\left(p^{-1} + \delta(d^*)\right) \sim p,$$
or $N^* \sim p/p_o^*$. Substituting this condition in (52) yields $p_o^* \sim \sqrt{pd^*/(2\lambda c R^2)}$, so $N^* \sim \sqrt{2\lambda c R^2 p/d^*}$. From (51), we obtain $\bar{D}^* \sim 2\sqrt{2d^* {\rm e} p^{-1} \lambda c R^2}$. Therefore, $d^* \sim 1$ and (30)-(32) follow.
- If $p_o^* = \Theta(1)$, it is necessary that $N^* d^* = \Theta(\lambda)$, otherwise, from (51) $\bar{D}^* = {\rm e}^{\Theta(\lambda)}$. Therefore, $\bar{D}^* = \Theta(\lambda)$. Since this scaling is worse than $\Theta(\sqrt{\lambda})$, this case is rejected, which concludes the proof.

2. $d^* = \Theta(N^*)$: From (33), it is necessary that $N^* = \Theta(\lambda T_o)$ for a non-vanishing p_s. From (35), it follows that $\bar{D}^* = \Theta(N^* d^*) = \Theta((\lambda T_o)^2)$. Since this scaling is worse than $\Theta(\lambda T_o)$, this case is rejected, which concludes the proof.

G. Proof of Proposition 13

Since Π_r is a PPP, we assume, without loss of generality, that the typical relay is located at the origin, i.e., $x = (0,0)$. Then $P'_{{\rm cr},2}$ can be written as

$$P'_{{\rm cr},2} = \frac{\mathbb{E}_{r_1, r_2, \theta}\left[{\rm e}^{-\lambda_r {\rm A}\left(B(z,r_1) \cup B(z', r_2)\right)\}}\right]}{\mathbb{E}_{r_1}\left[{\rm e}^{-\lambda_r {\rm A}(B(z,r_1))}\right]},$$

where $r_1 = |z|$, $r_2 = |z'|$, $\theta = \angle(z, z')$, $B(z, r_1)$ is the disc with center z and radius r_1, and ${\rm A}(\cdot)$ denotes area. If $\theta \in [0, \pi)$, geometric calculations lead to

$${\rm A}\left(B(z,r_1) \cup B(z', r_2)\right) = (\pi - \phi) r_1^2 + (\phi + \theta) r_2^2 + y r_1 \sin\phi,$$

where $y = |z - z'|$ and $\phi = \angle(z, z - z')$. For $N = 2$, by the displacement theorem [9], $\Pi_{r,{\rm ideal}}$ is a PPP with density λ. Therefore θ is uniformly distributed in $[0, 2\pi)$, the joint pdf of (r_1, r_2) is $f(r_1, r_2) = 4(\lambda\pi)^2 r_1 r_2 {\rm e}^{-\lambda\pi r_2^2}$, $r_2 > r_1$, and the pdf of r_1 is $f(r_1) = 2\lambda\pi r {\rm e}^{-\lambda\pi r_1^2}$, $r_1 > 0$. Performing the expectations over r_1, r_2, θ, taking into account the symmetry for $\theta \in [0, \pi)$ and $\theta \in [\pi, 2\pi)$, and making the change of variables $t_1 = \sqrt{\lambda\pi} r_1$, $t_2 = \sqrt{\lambda\pi} r_2$, we obtain (41).

REFERENCES

[1] M. Haenggi and D. Puccinelli, "Routing in ad hoc networks: a case for long hops," *IEEE Commun. Mag.*, pp. 93–101, Oct. 2005.

[2] F. Xue and P. R. Kumar, "Scaling laws for ad hoc wireless networks: an information theoretic approach," *series of Foundations and Trends in Networking, Now Publishers Inc.*, vol. 1, pp. 145–270, Jul. 2006.

[3] A. E. Gamal, J. Mammen, B. Prabhakar, and D. Shah, "Optimal throughput-delay scaling in wireless networks - part I: the fluid model," *IEEE Trans. Inf. Theory*, pp. 2568–2592, Jun. 2006.

[4] J. G. Andrews, S. Weber, M. Kountouris, and M. Haenggi, "Random access transport capacity," *IEEE Transactions on Wireless Communications*, vol. 9, no. 6, pp. 2101–2111, Jun. 2010.

[5] P. Gupta and P. R. Kumar, "The capacity of wireless networks," *IEEE Trans. Inf. Theory*, pp. 388–404, Mar. 2000.

[6] M. J. Neely and E. Modiano, "Capacity and delay tradeoffs for ad hoc mobile networks," *IEEE Trans. Inf. Theory*, pp. 1917–1937, Jun. 2005.

[7] J. Andrews *et al.*, "Rethinking information theory for mobile ad hoc networks," *IEEE Commun. Mag.*, pp. 94–101, Dec. 2008.

[8] E. S. Sousa and J. A. Silvester, "Optimum transmission ranges in a direct-sequence spread-spectrum multi-hop packet radio network," *IEEE J. Sel. Areas Commun.*, vol. 8, pp. 762–771, Jun. 1990.

[9] M. Haenggi, J. G. Andrews, F. Baccelli, O. Dousse, and M. Franceschetti, "Stochastic geometry and random graphs for the analysis and design of wireless networks," *IEEE Journal on Selected Areas in Communications*, vol. 27, no. 7, pp. 1029–1046, Sep. 2009.

[10] S. P. Weber, X. Yang, J. G. Andrews, and G. de Veciana, "Transmission capacity of wireless ad hoc networks with outage constraints," *IEEE Trans. Inf. Theory*, vol. 51, pp. 4091–4102, Dec. 2005.

[11] F. Baccelli, B. Błaszczyszyn, and P. Mühlethaler, "An Aloha protocol for multi-hop mobile wireless networks," *IEEE Trans. Inf. Theory*, vol. 52, pp. 421–436, Feb. 2006.

[12] ——, "On the performance of time-space opportunistic routing in multi-hop mobile ad hoc networks," in *IEEE WiOpt 2008*, Apr. 2008, pp. 307 – 316.

[13] R. K. Ganti and M. Haenggi, "Dynamic connectivity and path formation time in Poisson networks," *Wireless Networks*, 2013, accepted. Available at http://www.nd.edu/~mhaenggi/pubs/winet13.pdf.

[14] M. Haenggi, "On routing in random Rayleigh fading networks," *IEEE Trans. Wireless Commun.*, vol. 4, pp. 1553–1562, Jul. 2005.

[15] O. Oyman and S. Sandhu, "A Shannon theoretic perspective on fading multihop networks," in *CISS 06*, Princeton, Mar. 2006.

[16] M. Sikora, J. N. Laneman, M. Haenggi, D. J. Costello, and T. Fuja, "Bandwidth- and power-efficient routing in linear wireless networks," *Joint Special Issue of IEEE Transactions on Information Theory and IEEE Transactions on Networking*, vol. 52, pp. 2624–2633, Jun. 2006.

[17] D. Rajan, "Power efficient delay allocation in multi-hop wireless networks," *IEEE Trans. Veh. Technol.*, vol. 56, pp. 1813–1825, Jul. 2007.

[18] M. Xie and M. Haenggi, "A study of the correlations between channel and traffic statistics in multihop networks," *IEEE Transactions on Vehicular Technology*, vol. 56, pp. 3550–3562, Nov. 2007.

[19] ——, "Towards an end-to-end delay analysis of wireless multihop networks," *Elsevier Ad Hoc Networks*, vol. 7, no. 5, pp. 849–861, Jul. 2009.

[20] J. Hsu and P. P. Burke, "Behavior of tandem buffers with geometric input and Markovian output," *IEEE Transactions on Communications*, vol. 24, no. 3, pp. 358 – 361, Mar. 1976.

[21] M. Haenggi, "Outage, local throughput, and capacity of random wireless networks," *IEEE Transactions on Wireless Communications*, vol. 8, no. 8, pp. 4350–4359, Aug. 2009.

[22] M. Sidi and A. Segall, "Two interfering queues in packet-radio networks," *IEEE Trans. Commun.*, pp. 123–129, Jan. 1983.

[23] R. K. Ganti and M. Haenggi, "Spatial and temporal correlation of the interference in ALOHA ad hoc networks," *IEEE Communications Letters*, vol. 13, no. 9, pp. 631–633, Sep. 2009.

[24] R. Giacomelli, R. K. Ganti, and M. Haenggi, "Outage probability of general ad hoc networks in the high-reliability regime," *IEEE/ACM Transactions on Networking*, vol. 19, pp. 1151–1163, Aug. 2011.

[25] R. M. Corless, G. H. Gonnet, D. E. G. Hare, D. J. Jeffrey, and D. E. Knuth, "On the Lambert function," *Adv. Computational Maths.*, vol. 5, pp. 329–359, 1996.

[26] K. Stamatiou and M. Haenggi, "Random-access Poisson networks: stability and delay," *IEEE Communication Letters*, vol. 14, no. 11, pp. 1035–1037, Nov. 2010.

[27] G. Bianchi, "Performance analysis of the IEEE 802.11 distributed coordination function," *IEEE J. Sel. Areas Commun.*, vol. 18, pp. 535–547, Mar. 2000.

[28] S. Weber, A. Kini, and A. Petropulu, "A new approximation for slotted buffered Aloha," in *42nd Annual Conference on Information Sciences and Systems (CISS)*, 2008, pp. 1143–1148.

[29] M. Haenggi and R. Smarandache, "Diversity polynomials for the analysis of temporal correlations in wireless networks," *IEEE Transactions on Wireless Communications*, 2013, submitted. Available at http://www.nd.edu/~mhaenggi/pubs/twc14.pdf.

Kostas Stamatiou received his Diploma in Electrical and Computer Engineering from the National Technical University of Athens in 2000, and the M.Sc. and Ph.D. degrees in Electrical Engineering in 2004 and 2009, respectively, from the University of California San Diego (UCSD). From 2009 to 2010 he was a post-doctoral scholar in the Department of Electrical Engineering at the University of Notre Dame, South Bend, Indiana, and from 2010 to 2012 he held a research appointment at the Department of Information Engineering at the University of Padova, Italy. He currently holds a researcher position at the Centre Tecnològic de Telecomunicacions de Catalunya (CTTC), Barcelona, Spain. His research interests lie in the areas of wireless communications, stochastic geometry and random networks, and energy harvesting systems.

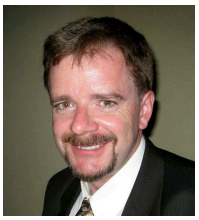

Martin Haenggi (S95, M99, SM04) is a Professor of Electrical Engineering and a Concurrent Professor of Applied and Computational Mathematics and Statistics at the University of Notre Dame, Indiana, USA. He received the Dipl.-Ing. (M.Sc.) and Dr.sc.techn. (Ph.D.) degrees in electrical engineering from the Swiss Federal Institute of Technology in Zurich (ETH) in 1995 and 1999, respectively. After a postdoctoral year at the University of California in Berkeley, he joined the University of Notre Dame in 2001. In 2007-2008, he spent a Sabbatical Year at the University of California at San Diego (UCSD). For both his M.Sc. and Ph.D. theses, he was awarded the ETH medal, and he received a CAREER award from the U.S. National Science Foundation in 2005 and the 2010 IEEE Communications Society Best Tutorial Paper award. He served an Associate Editor of the Elsevier Journal of Ad Hoc Networks from 2005-2008, of the IEEE Transactions on Mobile Computing (TMC) from 2008-2011, and of the ACM Transactions on Sensor Networks from 2009-2011, and as a Guest Editor for the IEEE Journal on Selected Areas in Communications in 2008-2009 and the IEEE Transactions on Vehicular Technology in 2012-2013. He also served as a Distinguished Lecturer for the IEEE Circuits and Systems Society in 2005-2006, as a TPC Co-chair of the Communication Theory Symposium of the 2012 IEEE International Conference on Communications (ICC'12), and as a General Co-chair of the 2009 International Workshop on Spatial Stochastic Models for Wireless Networks (SpaSWiN'09) and the 2012 DIMACS Workshop on Connectivity and Resilience of Large-Scale Networks, and as the Keynote Speaker of SpaSWiN'13. Presently he is a Steering Committee Member of TMC. He is a co-author of the monograph "Interference in Large Wireless Networks" (NOW Publishers, 2009) and the author of the textbook "Stochastic Geometry for Wireless Networks" (Cambridge University Press, 2012). His scientific interests include networking and wireless communications, with an emphasis on ad hoc, cognitive, cellular, sensor, and mesh networks.